A Study of the PDILT Protein and its Expression in Immortalised Cells and Tissues

ALEXANDER, MICHAEL,HUGH

A Study of the PDILT Protein and its Expression in Immortalised Cells and Tissues

Michael Hugh Alexander

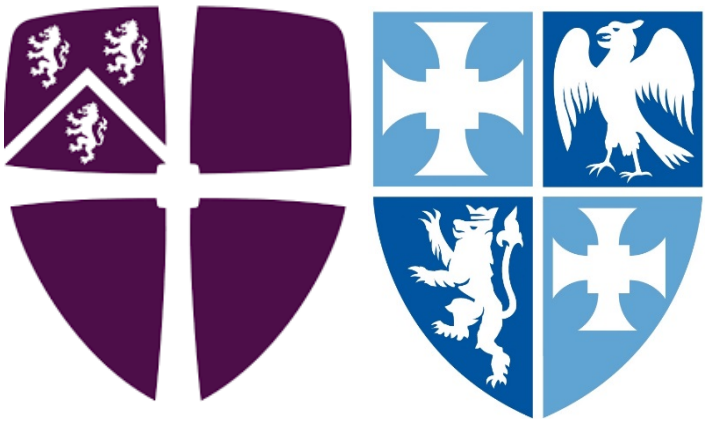

A Thesis Submitted for the Degree of Master of Science (By Research)
March 2018

Supervised by Dr. Adam Benham
Department of Biosciences
University of Durham
Durham
United Kingdom

A Study of the PDILT Protein and its Expression in Immortalised Cells and Tissues

MRes Thesis of Michael Hugh Alexander

Abstract

Protein Disulfide Isomerase-like protein of the Testis (PDILT) is an endoplasmic reticulum (ER) protein that is required for male fertility and is a member of the Protein Disulfide Isomerase (PDI) family. PDI has a well-established role in the formation of disulfide bonds in newly synthesised proteins, which is facilitated by thioredoxin active sites (a CXXC motif) in the **a** domains. PDILT, however, lacks these classic redox active sites and has an SXXS and a SXXC motif in the **a** and **a'** domain respectively but nevertheless interacts with clients in the ER. PDILT also contains a unique C-terminal extension, the function of which is unknown.

In order to examine the role that the unique structural elements of PDILT contribute to client binding, several PDILT mutant constructs were transfected into HT1080 cells and subjected to a series of western blotting and immunofluorescence experiments. In this thesis, data is shown to support the assertion that the two solvent-exposed cysteines present in PDILT mediate all disulphide dependent interactions with client proteins. We also show that the deletion of the C-terminal extension caused a large increase in client interactions and thus we theorise that the tail of PDILT regulates PDILT/client protein interactions.

PDILT is specifically expressed in the post-meiotic spermatid cells of the testis, which limits the potential to study the expression and function of endogenous PDILT in cell lines. Thus, work in this thesis has also examined a variety of immortalised cell lines for PDILT expression, to develop better systems for the further study of testis specific chaperones. Along with PDILT, a range of immortalised cell lines were also examined for the derepression of other testis specific ER chaperone proteins. As a result of this investigation, this thesis also reports on the unique expression of calmegin in cell lines with different genotypes.

Table of Contents

List of Figures and Tables

Table of Abbreviations

ADAM1 - A Disintegrin and Metalloprotease 1

ADAM2 - A Disintegrin and Metalloprotease 2

ADAM3 - A Disintegrin and Metalloprotease 3

AGR2 - Anterior Gradient Protein 2

APS1 - Autoimmune Polyendocrine Syndrome Type 1

ATF4 - Activating transcription factor 4

ATF6 - Activating Transcription Factor 6

BiP - Binding Immunoglobulin Protein (BiP)

BSA – Bovine Serum Albumin

CALR3 – Calreticulin 3

cDNA – Complementary DNA

CLGN - Calmegin

CNX – Calnexin

CNS – Central Nervous System

CTSB – Cathepsin B

CTSD – Cathepsin D

DMEM - Dulbecco's Modified Eagle's Medium

eIF2α - Eukaryotic Initiation Factor 2 Alpha

ECL - Enhanced Chemiluminescence

EndoPDI – Endothelial Protein Disulfide Isomerase

ER – Endoplasmic Reticulum

ERAD – ER-Associated Degradation

ERK - Mitogen-Activated Protein Kinase

Ero1α - Endoplasmic Reticulum Oxidoreductase 1 Alpha

ERp57 - Endoplasmic Reticulum Protein 57

ERp29 - Endoplasmic Reticulum Protein 29

FAD - Flavin Adenine Dinucleotide

FBS – Fetal Bovine Serum

GAMPO - Goat Anti-Mouse Peroxidase

GAPDH - Glyceraldehyde 3-Phosphate Dehydrogenase

GDP - Guanosine Diphosphate

GI28/21 - gi:28372543/gi:21757251 (Hypothetical Protein)

GRB2 - Growth Factor Receptor-Bound Protein 2

GSBP - Glycosylation Site Binding Protein

Grp78 - 78 kDa Glucose-Regulated Protein

GRP94 - Heat Shock Protein 90kDa Beta Member 1

GRP170 - Glucose-Regulated Protein 170

GTP - Guanosine Triphosphate

Ire1 - Inositol-Requiring Enzyme 1

MEK – Mitogen-Activated Protein Kinase Kinase

NR – Non-Reducing

PACMA 31 – PDI Inhibitor III

PBS – Phosphate Buffered Saline

PC1 - Proprotein convertase 1

PC2 - Proprotein convertase 2

PDI – Protein Disulfide Isomerase

PDIA1 – Protein Disulfide Isomerase

PDIA3 – Protein Disulfide Isomerase Family A Member 3

PDIA6 - Protein Disulfide Isomerase Family A Member 6

PDILT – Protein Disulfide Isomerase-like protein of the Testis

PDIp – Protein Disulfide Isomerase of the Pancreas

PERK - Protein Kinase R (PKR)-like Endoplasmic Reticulum Kinase

PVDF - Polyvinylidene Difluoride

P4HB - Beta-Subunit of Prolyl 4-Hydroxylase

P53 – Cellular Tumor Antigen p53

R – Reducing

RTK – Receptor Tyrosine Kinase

SARPO – Swine Anti-Rabbit Peroxidase

SDS-PAGE - Sodium Dodecyl Sulfate Polyacrylamide Gel Electrophoresis

SOS – Son of Sevenless

S1p - Membrane-Bound Transcription Factor Site-1 Protease

S2p - Membrane-Bound Transcription Factor Site-2 Protease

TBS - Tris Buffered Saline

TBS-T - Tris buffered saline with Tween

UPR – Unfolded Protein Response

VEGF - Vascular Endothelial Growth Factor

WT – Wild Type

XBP1 - X-box Binding Protein 1

Declaration

I declare that the contents and all data presented in this thesis is the result of my own work. No part of the material offered has previously been submitted for a higher degree. The body of work has been achieved under the supervision of Dr. Adam Benham.

Michael Hugh Alexander

March 2018

Acknowledgements

I would like to thank Dr. Adam Benham for supervising me over the course of my masters. Not only has he had incredible patience but also has opened up numerous opportunities to me. I would also like to thank Naomi Carne, Steven Bell and Sarah Francis for their help in the laboratory and also providing endless support whenever I asked for it.

I would also like to thank Prof. Penny Lovat for the generous gift of the melanoma cell lines, melanocyte cells and human melanoma tumours that were used in this thesis but also for allowing me to spend a considerable amount of time in her laboratory. I would also like to thank Dr. David Hill for providing my training whilst in Prof. Lovat's laboratory.

I would also like to thank Dr. Maria Christina W. Avellar for inviting me to spend time in her laboratory and also to attend the 49TH SBFTE Conference.

Finally, I would like to thank my family for their support, both emotional and financial, over the course of my masters.

1. Introduction

1.1. The Endoplasmic Reticulum

The endoplasmic reticulum (ER) ensures that secreted or secretory pathway proteins produced by the cell are correctly folded and modified. The ER facilitates this folding of newly synthesised proteins at several different levels. The first level of screening comes from general error checking by a series of major molecular chaperones. These chaperone proteins, such as BiP/GRp78 are able to detect obvious defects in protein folding, such as the expose of hydrophobic areas. Once the defects have been detected, these proteins are able to facilitate refolding of the protein to its correct shape and also stops the protein from being secreted. A secondary level of error checking is also present in the ER, but is much more specific than the previous level and checks specific protein families. In a similar fashion to the previous level of error checking, the binding and activity of these proteins prevents export of the client proteins. The ER also contains a complex sorting system that is able to separate proteins according to their folding state, with correctly folded proteins being localised to specific areas for export and incorrectly folded proteins being targeted for degradation via ER-associated degradation (ERAD) (Ellgaard and Helenius 2001). This quality control system is designed to ensure that only correctly folded proteins can exit the ER and any incorrectly folded proteins are destroyed before they can aggregate and cause damage to the cell (Ellgaard, Helenius 2001).

Protein disulfide isomerase (PDI) and its homologues have been identified as key proteins involved in the protein folding process. PDI catalyses the formation of disulphide bonds in newly synthesized proteins, but can also work as a general chaperone. PDILT is a relatively newly identified homologue of the PDI family, and was cloned by van Lith et al. 2004. PDILT has been found to localise to the testis and is required for male fertility.

1.2. The PDI Family of Proteins

One of the many folding mechanisms used to stabilise protein structure is the formation of disulphide bonds. PDI is a key protein involved in this process. This abundant 55 kDa protein has two main roles, namely oxidation/reduction, and the isomerisation of disulfide bonds in nascent proteins. PDI is a member of the thioredoxin superfamily but has several family members in humans, with these family members summarised in Table 1. PDIs and other members of the thioredoxin superfamily are characterised by having a CXXC motif in the

active site. PDI contains this classical thioredoxin active site within its a and a' domain. The protein also contains two other domains, the b and b' domains, that are catalytically inactive. A diagrammatic representative of PDIs structure is presented in Figure 1. PDI has several mammalian homologues that are localised to the ER, all of which have slight variations in structure but all contain at least one thioredoxin-like domain (Benham et al. 2013).

1.3. PDI Key Functions

The oxidation/reduction activity of PDI relies on the active site being able to exist in two forms, an oxidised form or a reduced form. The oxidised form is when the cysteines in each active site are linked via a disulfide bond and the reduced state is when the cysteines exist in a dithiol state. PDI is able to cycle between these two states by being oxidised and reduced and in doing so, can oxidise or reduce other substrates, breaking or forming disulphide bonds. The process of disulphide bond formation occurs by a redox pathway, which is summarised in Figure 2. It can be seen in Figure 2 that the Ero1α protein plays a key role in this cycling of oxidation and reduction that ultimately leads to disulphide bond formation. Ero1α is able to donate disulphide bonds to PDI, which then allows PDI to induce disulphide bond formation in client proteins. This however causes electron flow in the opposite direction, where an electron passes from PDI to Ero1α to molecular oxygen. Via utilising the FAD cofactor, molecular oxygen is reduced to peroxide, which is processed within the ER via peroxiredoxin IV, which acts to detoxify the molecule (Szarka and Bánhegyi 2011).

The process of disulphide formation can be error prone, due to the multiple ways cysteines can be disulfide-bonded within the same protein, as can be seen in Figure 3. As a result, these bonds often need to be corrected and PDI has isomerisation activity that facilitates these corrections. PDI is able to do this via one of two routes; the intramolecular route, or via cycles of oxidation and reduction. The intramolecular route allows PDI to directly attack a target cysteine and disrupt the disulphide bond it has formed. The bonds within the protein can then be rearranged or be reformed. The second route is via a repeated cycle of oxidation and reduction of the substrate that causes random rearrangement of the disulphide bonds until the correct protein structure is formed. These two routes allow for PDI to mediate the correct disulphide bond formation on newly synthesised proteins (Wilkinson, Gilbert 2004).

Table 1: The Mammalian Protein Disulphide Isomerase Family			
Name of Protein	**Domain Arrangement**	**Active Site Sequence**	**Protein Length**
PDI (PDIA1)	abb′xa	CGHC, CGHC	508
PDIp (PDIA2)	abb'xa	CGHC, CTHC	525
ERp57 (PDIA3)	abb'xa	CGHC, CGHC	505
ERp72 (PDIA4)	a^{o}abb′xa′	CGHC. CGHC, CGHC	645
PDIR (PDIA5)	ba^{o}aa′	CSMC, CGHC, CPHC	519
P5 (PDIA6)	aa'b	CGHC, CGHC	440
PDILT	abb'xa'	SKQS, SKKC	584
ERdJ5	Jabbaaa	CSHC, CPPC, CHPC, CGPC	793
ERp44	abb'	CRFS	406
ERp46	a^{o} aa′	CGHC, CGHC, CGHC	432
ERp18	a	CGAC	172
ERp27	bb'	-	273
ERp29	b'D	-	261
TMX	a	CPAC	280
TMX2	a	SNDC	296
TMX3	abb'	CGHC	454
TMX4	a	CPSC	349
hAGR2	a	CPHS	175
hAGR3	a	CQYS	166
ERp90	Trz1-5	-	825

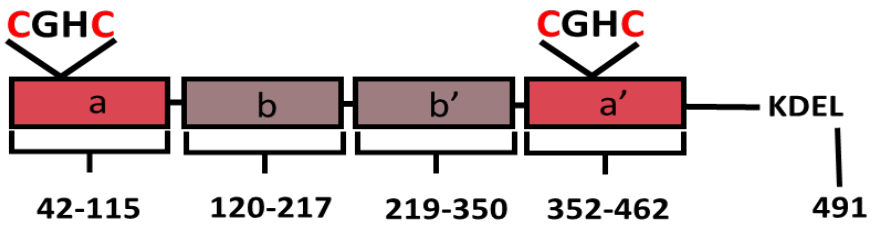

Figure 1. **The Domain Organisation of PDI**. A diagrammatic representation of the domain organisation of PDI.

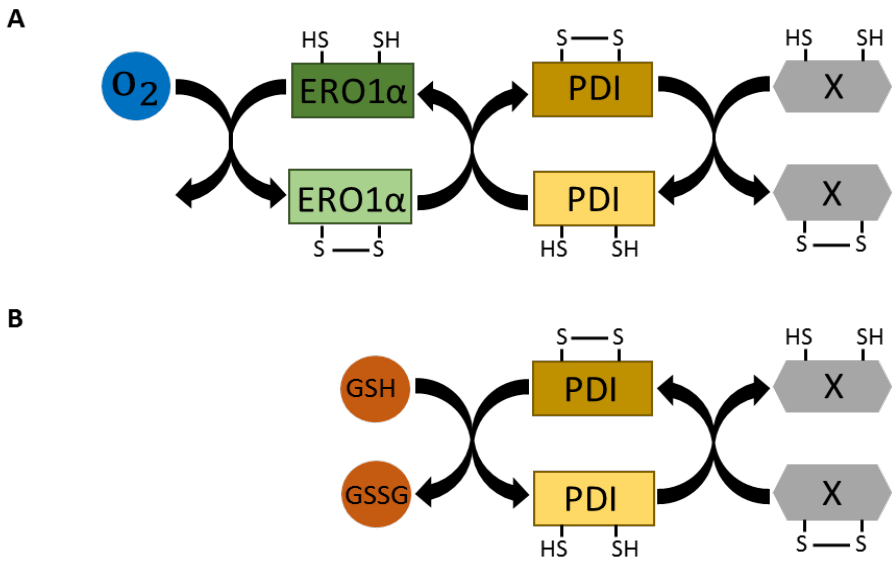

Figure 2. The Process of Oxidation and Isomerisation Mediated by PDI. (**A**) The process of oxidation that leads to the formation of disulphide bonds in newly formed proteins. (**B**) The process of isomerisation that allows PDILT to break incorrectly formed disulphide bonds in incorrectly folded proteins.

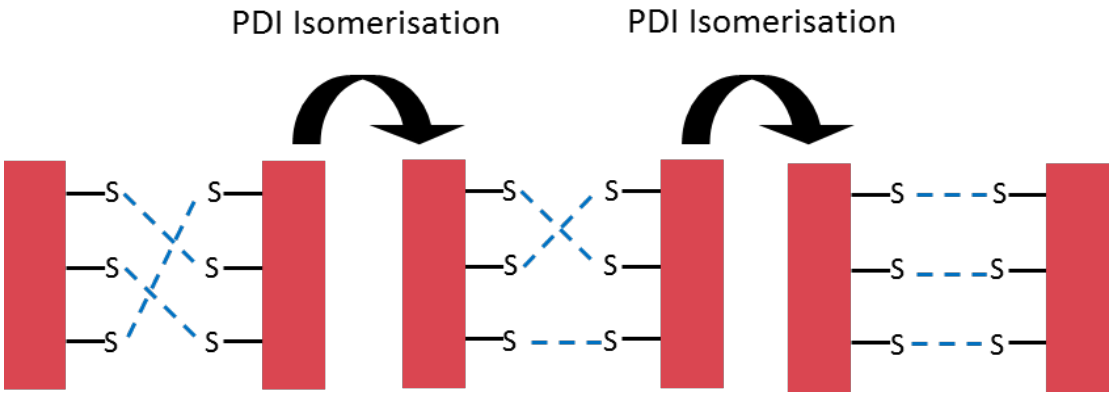

Figure 3. Intra-molecular Disulphide Bond Rearrangement. A diagrammatic representation of the many different configurations of disulphide bonds that are possible within the same protein, showing the need for PDIs isomerisation activity to ensure the correct configuration of disulphide bonds form.

1.4. PDI Additional Functions

PDI performs a number of other functions in the ER. It has been shown that the β subunit of the enzyme prolyl-4-hydroxylase is PDI, which facilitates the hydroxylation of collagen. PDI has also been reported to have chaperone activity on non-disulfide containing proteins, as it has been shown that when GAPDH, a protein that contains no disulphide bonds, is incubated with PDI, this increases reactivation of GAPDH and decreases its aggregation. (Cai et al. 1994).

1.5. PDILT Discovery

Whilst PDI has been studied to a great extent, homologues of this protein are less well investigated. These homologues include PDIp, which has been found to be specifically localised to the pancreas, and EndoPDI, which specifically localises to endothelium tissue. PDILT, another PDI homologue, was discovered using a database-BLAST search approach, with PDI as the input sequence (van Lith et al. 2004). The PDILT gene was initially termed GI28/21, which shared 27 % identity and 48 % similarity with PDI. The protein encoded by this gene has an unusual abb'a' domain arrangement, but lacks the redox active motifs (CXXC), instead having SSKQS (SXXS) and WSKKC (SXXC) in the a and a' domains respectively. In addition to this difference, GI28/21 also has a free cysteine at position 135 and both N and C-terminals are altered compared to PDI. The N-terminus has a small insertion and the C terminus has an extension that increases the size of this protein to 67 kD (van Lith et al. 2004).

1.6. PDILT Expression and Localisation

The expression and localisation of this unusual protein was then examined (van Lith et al. 2004). This was achieved by RT-PCR, western blotting and immunohistochemistry using several different mouse tissues. The only tissue that returned a positive identification of GI28/21 was mouse testis tissue. Several human tissue lines were also analysed with none showing GI28/21 expression. Analysis of testis derived Sertoli SK11 cells also showed they did not express GI28/21. With this expression data, the protein was renamed protein disulfide isomerase like protein of the testis (PDILT). As no cell lines to date express PDILT endogenously, Myc tagged PDILT constructs were transfected into HeLa cells to study its intracellular localisation. Immunostaining and confocal microscopy revealed PDI and PDILT had overlapping staining, indicating that PDILT resides in the ER. To determine the

glycosylation state of PDILT and provide further evidence of its localisation, a PDILT transfected cell lysate was subject to treatment with Endoglycosidase H (Endo H), which can only digest immature N-glycans in the ER. When subject to western blotting, PDILT increased mobility, moving from 76 kD to 65 kD after Endo H digestion. These results prove that PDILT is an ER resident glycosylated protein. The work by van Lith et al. 2007 defined the cell-specific location of PDILT within the testis. This was done by immunohistochemistry of sections of testis derived from rat, mouse, human, marmoset and macaque. It was found that in rat, mouse and macaque seminiferous tubule sections, the germ cells were heavily stained. The other tissues, human and marmoset, had more complex staining but within similar testis cell areas. This specific expression pattern is unique, in comparison to other PDI homologues, which have been shown to have broad expression across all cell types within the testis.

The germ cells that show expression of PDILT were found to be at stage VII of maturation, which marks when the germ cells begin to differentiate. All species were found to express PDILT once the meiotic division had occurred. This observation, combined with the observation that PDILT was not present in spermatozoa, led to the hypothesis that PDILT was linked to germ cell development and that its expression was temporally controlled. To test this, testis tissues from rodents at different ages were subject to RT-PCR to test for PDILT expression. PDILT mRNA wasn't detected in the testis until 30 days of age, and had maximum expression by day 45. Interestingly, when the testis was examined for the expression of the testis-specific ER resident chaperone calmegin (CLGN), it was found to overlap with the appearance of PDILT in the testis. To determine whether the onset of protein expression mirrored the onset of gene expression, western blotting was performed. It was found that the PDILT protein appeared at day 30 and reached the maximum by day 45, whilst CLGN reached maximum expression from day 30. This was confirmed with immunostaining of testis sections taken from rodents at different ages, which showed that PDILT positive germ cells only appeared at day 31 in the seminiferous tubules. These results taken together show that PDILT expression is tied to the formation of round spermatids (stage VII) and is also co-ordinated with the expression of CLGN (van Lith et al. 2007).

1.7. PDILT Activity

It has been well documented that PDI forms disulfide bonds with both client and partner proteins as part of its oxidative cycle, so to establish whether PDILT forms similar complexes, pulse-chase and western blotting experiments were carried out under reducing and non-reducing conditions on cells transfected with PDILT. Under non-reducing conditions, it was

shown that higher molecular weight complexes do form, suggesting that PDILT does interact with other proteins. The identity of these proteins remains unknown, although one of these complexes is likely to be a PDILT dimer. Comparison between the reducing and non-reducing gels showed that the monomeric form of PDILT doesn't form a disulphide bond between the SXXC motif in the a' domain and non-active cysteine at position 135, as no difference in mobility was detected upon western blotting. Both of these observations were found to be true *in vivo*, as PDILT from mouse testis lysate showed a similar banding pattern. To determine the roles of the conserved free cysteines in PDILT, van Lith et al. 2007 transfected cell lines with PDILT mutants (C135A, C420A and the C135A/C420A double mutant) and analysed transfectant lysates on a western blot, under reducing and non-reducing conditions, to see if these cysteines were required for complex formation. Both of the single substitution PDILT mutants caused a reduction in the molecular weight of the higher molecular weight complexes and the double mutant abolished all interactions, indicating that both cysteines are solvent exposed and involved in protein interactions (van Lith et al. 2007).

In order to see if PDILT shared any other similar interactions with PDI, it was then investigated if PDILT could also interact with Ero1α, as this would help establish whether redox activity is required for a PDI protein to interact with an Ero1 protein. Co-immunoprecipitation of transfected Ero1a and PDI did show that they could interact, although such an interaction may not occur functionally *in vivo.* To examine whether PDILT had any oxido-reductase activity *in vitro*, an insulin reduction assay was used. Incubating insulin with PDI and PDILT, respectively, and comparing whether the insulin B chain precipitates is indicative of reductase activity. For PDI the insulin B chain precipitated out, as expected from previous studies (Watanabe et al. 2014). In contrast, PDILT did not catalyse the reduction of insulin, suggesting that PDILT does not have classical oxidoreductase activities.

The crystal structure of PDILT has now been solved. Initially, only the b' domain of PDILT was crystallised, which revealed the presence of a hydrophobic pocket, which is likely the site of substrate binding (Bastos-Aristizabal et al. 2014). However, in 2017, the crystal structure of full-length PDILT was solved to a 2.4 Å resolution. This structure confirmed the observation of a hydrophobic pocket in the b' domain but also provided evidence that the C terminal tail is vital for the chaperone activity of PDILT (Yang et al. 2018).

1.8. PDILT and Male Fertility

One study, Ellerman et al. 2006, has the PDI family to the mechanism of sperm/egg membrane fusion, showing that a variety of PDI inhibitors reduced both fertilisation rate and fertilisation index. This paper suggested that ERp57 could operate at the sperm cell surface to provide oxido-reductase activity for sperm adhesion proteins. However, the inhibitors and antibodies used in these experiments were not specific to ERp57, and it remains possible that other oxido-reductase activities are required for sperm-egg binding. Since PDILT is present within the testis, and is not thought to be present in the sperm, it is unlikely to have the same role as ERp57. How PDILT links to male fertility was indicated in a study of CLGN and calsperin (CALR3), which are germ cell specific homologues of ER resident lectin chaperones. These two proteins assist the maturation of a select group of ADAMs, key proteins in male fertility that are required for correct sperm migration and sperm egg adhesion. CLGN itself is required for the dimerization of ADAM1A/ADAM2 and CALR3 is required for the maturation of ADAM3. PDILT interacts with both CLGN (van Lith et al. 2007) and CALR3 (Tokuhiro et al. 2012), indicating that these chaperones work together in male fertility. Proof of these interactions was found by subjecting testis and liver lysates to immunoprecipitation with either an anti-CLGN or an anti-PDILT antibody, with the resulting lysate being analysed by western blotting and stained for co-immunoprecipitating CLGN and PDILT. Both immunoprecipitated lysates contained CLGN and PDILT, showing that PDILT does interact with CLGN. Further work showed that PDILT interacted with CLGN and CALR3 and that it interacted with ADAM3 but not ADAM1/2 via a series of immunoprecipitation and western blot experiments. In tissue from *Pdilt-/-* male mice, it was noted that whilst ADAM1/2 heterodimerization was still present, ADAM 3 disappeared from spermatozoa when PDILT was knocked out. To try and explain this, testis and epididymal cell lysates were subject to western blotting and it was noted that ADAM3 was present on maturing sperm cells until the caput epididymis, suggesting that lack of PDILT causes loss of ADAM3 from the spermatozoa at a late stage of maturation (Tokuhiro et al. 2012).

To further explore the impact of these specialised ER chaperone proteins on Adam3 maturation, several knock out mice were analysed. These knockout mice had their Pdilt, Clgn and Calr3 genes disrupted. A trypsin digest was then performed on mutant spermatozoa isolated from these knockout mice, to see which Adam proteins were expressed on the surface membrane. Whilst sperm from wild type and $Clgn^{-/-}$ had both Adam2 and Adam3 proteins on their surface, it was found that $Calr3^{-/-}$ and $Pdilt^{-/-}$ spermatozoa both lacked Adam3 on their surface. It was then asked whether Clgn, Calr3 and Pdilt participated in the

folding of Adam3. To do this wt, *Clgn*$^{-/-}$, *Calr3*$^{-/-}$ and *Pdilt*$^{-/-}$ spermatogenic cell membrane proteins were separated into detergent depleted or enriched samples and run on SDS-PAGE under reducing or non-reducing conditions. Under non-reducing conditions, the Adam3 protein was in a doublet, with the compact oxidised form being strongest in wt and *Clgn*$^{-/-}$ tissue but far weaker in the *Calr3*$^{-/-}$ and the *Pdilt*$^{-/-}$ mutants, thus suggesting that Pdilt and Calr3 have a role in the oxidative folding of Adam3 disulphide bonds. Whilst this shows clear evidence of Pdilts involvement in the maturation of Adam3, it did not demonstrate direct oxidoreductase activity. The consequence of a lack of Pdilt is male infertility, as when both male and female *Pdilt*$^{-/-}$ mice were mated with wt partners, only the males presented with infertility. To explore this observation further, green florescent protein was inserted transgenically into *Pdilt*$^{-/-}$ sperm and the sperm observed post-mating in the female reproductive tract, where they failed to enter the oviduct, despite showing normal mobility. This issue could be bypassed by inserting capacitated spermatozoa directly into the oviduct, which allowed for the production of healthy offspring. Interestingly, when *Pdilt*$^{-/-}$ spermatozoa were added to cumulus-free ZP-intact eggs, it was found that the spermatozoa had a low binding rate. However, fertilisation could be achieved with these mutant spermatozoa in the presence of cumulus conditioned media or with cumulus-free eggs. Thus cumulus cells have a previously under-estimated role in fertility and the factor(s) that help sperm bypass the requirement for Pdilt have yet to be identified (Tokuhiro et al. 2012).

1.9. PDILT Beyond the Testis

The impact PDILT has on male fertility has been extensively studied but there are hints that PDILT may be expressed beyond the male germ cells. For example, PDILT has been detected in seminiferous fluid (C. Avellar, personal communication) and has been identified as a genetic variant in a meta-analysis of factors that influence uromodulin expression, suggesting that PDILT may be expressed by specialist kidney cells (Olden et al. 2014). PDILT also becomes derepressed in patients with the rare autoimmune disease Autoimmune polyendocrine syndrome type 1 (APS1) (Landegren et al. 2016). Observation of data held at the Human Protein Atlas also suggests that PDILT may be expressed in certain pathologies, including in melanomas (https://www.proteinatlas.org). This is based on staining with a PDILT antibody (Sigma-Aldrich HPA041913) that has yet to be validated, and may potentially cross react with other PDI proteins. The Human Protein Atlas is a Swedish project that began in 2003 with the aim of mapping all known human proteins to their tissue of origin. One of the arms of this project is to analyse protein expression levels in cancer. When this project investigated a variety of cancer tissues for PDILT using the PDILT antibody (Sigma-Aldrich

HPA041913), there was some immunoreactivity in the cytoplasmic and nuclear compartment of several cancers, with some of the largest immunoreactivity found in melanoma. This suggestion that PDILT might be found in certain cancers leads to the possibility that PDILT may provide a growth advantage or promote metastatic activity of those tumours. This possibility is realistic, as numerous studies have found that that ER stress and ER proteins play an active role in the maintenance and development of cancer, as discussed below.

1.10. Cancer and ER Stress

The connection between the ER and pathology has been well researched, as many pathological conditions are known to cause disruption to the normal functioning of the ER, such as Alzheimer's disease, Type 2 Diabetes and a variety of cancers (Ozcan and Tabas 2012). How this deregulation occurs is different in different pathologies, but there are ultimately three ways pathologies are able to effect the ER. The first is via increasing the expression of key ER proteins, such as the increased expression of GRP 78/BiP and GRP94 observed in breast, lung and colon cancers (Moenner et al. 2007). Another effect is via changing post-translational modifications on ER proteins, such as the selective cleavage of PC1 and PC2 convertases, deregulating these proteases in liver metastasis (Tzimas et al. 2005). Finally, some pathologies are able to induce ER proteins that are normally localised solely to the ER to become secreted, such as the identification of Calreticulin in hepatocellular carcinoma patients (Le Naour et al. 2002). This alteration of the normal functioning of the ER can be expected in cancer. The ability of the cancer cell to manage ER homeostasis is key to its survival, as a failure in ER processing can lead to triggering of the unfolded protein response (UPR), which can ultimately lead to cell death by apoptosis. The and nutrient starved conditions often seen in cancer microenvironments can lead to ER stress. Thus the ability of a cancer to manage ER stress and the UPR is vital to ensure the survival of the cancer cell (Moenner et al. 2007).

The UPR is mediated by three proximal sensors: PERK, ATF6 and Ire1. How these proximal sensors trigger the UPR is depicted in Figure 4. PERK is a serine threonine kinase and acts to reduce the load of unfolded proteins in the ER. It stops the general translation of proteins, which otherwise would enter the ER and add to the aggregation of unfolded proteins. Interestingly, when a dominant negative PERK was forcibly expressed in MEF cells, these cells became more likely to die from hypoxic stress, suggesting that cells use PERK as survival signal to maintain normal function during times of cell stress (Meixia et al. 2005). The second

proximal signal is IRE1, which upon dimerization and phosphorylation causes the splicing of the XPB1 mRNA, which then leads to the production of the XBP1 protein. XBP1 then activates UPR linked target genes. Similar to PERK, when expression of IRE1 is silenced in a variety of cells, these cells are sensitised to death by hypoxia compared to wild type cells. This demonstrates the importance of this protein in determining the outcome of ER stress. The final proximal sensor is ATF6, which upon activation and translocation to the Golgi is cleaved by two related proteases, S1P and S2P. The release of a cytosolic fragment of ATF6 with transcription factor activity causes the activation of key genes involved in managing ER stress when truncated ATF6 enters the nucleus (Merksamer and Papa, 2010).

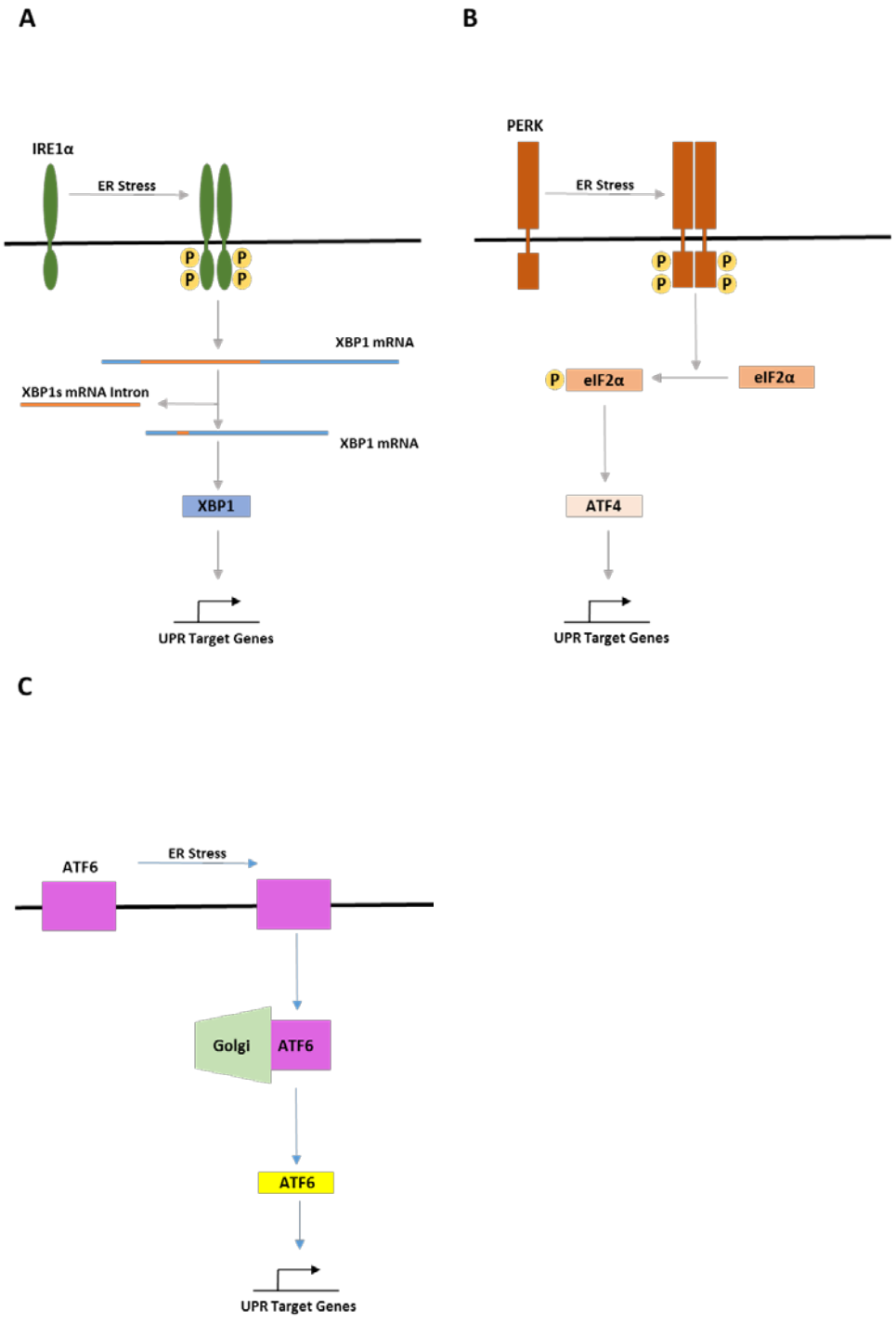

Figure 4. Signalling Pathways that Trigger the UPR. (**A**) Summary of the IRE1α signalling cascade. (**B**) Summary of the PERK signalling cascade. (**C**) Summary of the ATF6 signalling cascade.

The significance of these proteins in managing ER stress, shown by how easily cells can be pushed into apoptosis when these proteins are absent, demonstrates how this protein machinery can be exploited by cancer as a survival mechanism. UPR transcription factors, specifically AFT6 and XBP-1, have been found to be upregulated in hepatocellular carcinoma and is likely to be a protective response (Masahiro et al. 2003). Interestingly, these aren't the only proteins linked to the ER to undergo upregulation upon the development of cancer. Two more examples are GRP170 and ERp29. ERp29 is a small member of the PDI family whereas GRP170 is an ATPase which is normally involved in the release of VEGF, a protein that stimulates angiogenesis. The upregulation of GRP170 by cancer is used to ensure the complete protein folding and secretion of VEGF, as a mechanism of re-establishing a blood supply (Ozawa et al. 2001).

Whilst PDILT has never been examined at the molecular level to see if it is upregulated in cancer, other members of the PDI family, in addition to ERp57, have been widely studied and have been found to play key roles in cancer progression (Samanta et al. 2017).

1.11. The PDI Family and Cancer

Of all the members of the PDI family, AGR2 probably has the strongest relationship to cancer development. AGR2 was originally identified in *Xenopus laevis* and has strong expression in endoderm derived organs, especially in mucus producing and secreting cells. Indeed, the *Agr2-/-* mouse is deficient in mucus production and is susceptible to gastro-intestinal disease because of a defect in mucin quality control (Park et al. 2009). AGR2s role in cancer has been studied in a number of systems. Clonogenic assays performed on a variety of breast cancer cell lines have shown that the expression of AGR2 increased cancer cell survival and did not inhibit cell growth (Hrstka et al. 2010). Silencing AGR2 also inhibited invasion, proliferation and survival of breast cancer cell lines.

One of the mechanisms by which cancers utilise ER proteins for survival is by inducing resistance to classical cancer treatments. An example of this comes from breast cancer, where the AGR2 promotor is activated by oestrogen. This then leads to resistance of breast cancer cells to the classical treatment tamoxifen, as this treatment induces pro-survival genes. To understand which genes were being induced, a proteomic study of genes upregulated upon tamoxifen treatment was conducted. It found AGR2 to be the second highest induced protein. A chromatin immunoprecipitation analysis confirmed the activation of AGR2 by tamoxifen, as elevated levels of the alpha oestrogen receptor were found bound to the promoter of ARG2 when in the presence of tamoxifen, showing that it is induced by

cancer as a survival mechanism (Chevet et al. 2013). AGR2 has also been shown to play an important role in oesophageal cancer, as it was found to be significantly upregulated during the metaplastic epithelium stage of oesophageal cancer progression. It was then found that AGR2 acts to inhibit p53, an important cancer inhibitory protein (Chevet et al. 2013). These two specific examples demonstrate that AGR2 is strongly upregulated during the development of particular cancers. The exact mechanisms that allow AGR2 to support cancer growth are unknown, but it has been suggested that AGR2 ensures the correct processing of newly synthesised proteins, preventing the UPR response and thus preventing self-induced cell death (Higa et al. 2011).

AGR2 may contribute to the shift of a cancer to metastasis. One of the clearest examples is that grafted cancers that overexpress AGR2 have a higher likelihood to metastasize, when transplanted into nude mice models. The molecular mechanism of how AGR2 decreased the adhesion and increased the invasion of cancer cells was studied in pancreatic ductal adenocarcinoma. The expression of AGR2 was present across all stages of tumour development, and was localised both to the cytoplasm and at the surface of the cell membrane. The finding that AGR2 can be localised to the surface of the cell concurs with observations in breast cancer. By comparing two cell lines, one that overexpresses AGR2 and one subject to AGR2 silencing, AGR2s effect on metastasis could be studied. As expected, the cell line with upregulated AGR2 had an increased rate of invasion and the cell line with silenced AGR2 had a reduced rate of invasion. The key genetic finding of this study was that the proteases Cathepsin B (CTSB) and Cathepsin D (CTSD) were upregulated, which are proteases linked to highly invasive cancer. These observations show that AGR2 also has a role in cell migration and adhesion, as well as the role in maintaining ER health (Dumartin et al. 2011).

AGR2 isn't the only PDI family member that has been linked to invasiveness of a cancer cell. PDIA6 (P5), an aa'b redox active PDI homolog, was also studied in relation to glioblastoma multiforme (Goplen et al. 2006). Glioblastoma multiforme is another highly aggressive cancer that kills patients, typically within a year. Because of this hyper-aggressiveness, identifying genetic markers which determine aggressiveness is key to patient management and treatment. In order to identify these markers, an unusual xenotransplantation model of glioblastoma was established. It was noted that cancer spheroids on their initial transplantation into the CNS of nude mice had a phenotype with high invasiveness and low angiogenesis but when serially transplanted into nude mice, switched phenotype and were found to have low invasiveness with a high level of angiogenesis. These two phenotypic

qualities allow for a comparison between cancer cells from the same donor. The upregulated proteins from each phenotype were subject to mass spectrometry and identified. PDIA6 was one of the proteins identified in both phenotypes, but was found to have expression throughout the whole of the tumour in the highly invasive phenotype and only at the periphery in the low invasive phenotype. PDIA6 was also found at the surface of the cell using flow cytometry. Thus it is possible that PDIA6 acts at the cell surface to encourage cell migration. To investigate this, a PDI inhibitor was applied to both types of spheroid. This caused a decrease in invasive behaviour. The study went on to suggest that PDI acts at the cell surface by altering the conformational form of β3 integrin, as when this adhesion protein was blocked by an antibody, it also caused a reduction in invasive behaviour (Goplen et al. 2006).

Numerous studies show a clear correlation between higher expression of members of the PDI family and cancer (Samanta et al. 2017). Not only has it been demonstrated that they are upregulated to maintain ER integrity and stop UPR proapoptotic signalling (Higa et al. 2011), it has also been shown to play an active role at the surface of the cell, in reducing cell adhesion and promoting tumour migration (Dumartin et al. 2011). Thus, PDILT should also be considered as a candidate protein that is subject to upregulation via cancer mechanisms as a way to ensure tumour survival and invasion.

1.12. The PDI Family as a Target for Cancer Treatment

Whether targeting PDI can be effective in cancer treatment was explored in Lovat et al. 2008. This study explored the theory that cancer cells can be pushed into apoptosis by inhibition of PDI, as this leads to increased ER stress and UPR induced apoptosis. Firstly, the study demonstrated that ER stress could be induced in a variety of human melanoma cell lines with Fenretinide and Bortezomib. Fenretinide acts to induce ER stress through the generation of reactive oxygen species (ROS) (Mody and Mcilroy 2014) and Bortezomib acts to induce ER stress through inhibiting the proteasome, causing an aggregation of misfolded proteins within the ER, ultimately causing ER stress (Nawrocki et al. 2005). When ER stress had been validated, the impact of bacitracin, a PDI inhibitor, was investigated. It was found that when bacitracin was the only chemical incubated with the melanoma cell lines it didn't increase apoptosis of the melanoma cells. However, when bacitracin was incubated with Fenretinide or Bortezomib, there was an increase in cell death by apoptosis. This showed that when melanoma cells experience ER stress, they can be driven into apoptosis by inhibiting key ER proteins, in this case, PDI. To prove that bacitracin inhibition of PDI was the cause of the increase in cell death, P4HB (gene name of PDI) was transfected into the

melanoma cell lines, either in a redox active from or in a redox inactive form. Exogenous PDI prevented the increased cell death observed when bacitracin was incubated with either Fenretinide or Bortezomib. This is likely caused by the transfected PDI competing for binding to bacitracin, allowing PDI to facilitate cell survival. This effect was not seen when the inactive PDI was transfected into the melanoma cell lines. This highlights the importance of PDI in cancer cell survival during ER stress and also demonstrates that targeting PDI can have therapeutic potential (Lovat et al. 2008).

Although the full mechanistic detail of PDI family function in cancer is incomplete, clinical investigations into the link between PDI and cancer have been undertaken. An analysis carried out on published microarray data found that, compared to normal tissue, PDI is significantly upregulated in a number of cancers, such as lymphoma, ovarian and prostate cancers. PDI has also been found to be associated with the development of drug resistance during cancer treatment. For example, comparison of Aplidin resistant HeLa-R to Aplidin sensitive cells shows Aplidin resistant cells have a much higher level of PDI expression. When PDI is inhibited by direct treatment, the cells become re-sensitised to the treatment. PDI has also been linked to the maintenance of cancer cells. Several synthetic compounds have also been developed as inhibitors of PDI, with a view to using them in cancer treatment. These include Propynoic Acid Carbamoyl Methyl Amides (PACMA 31), an irreversible inhibitor of PDI, and 16F1, which targets both PDIA1 and PDIA3 (Xu et al. 2014).

Combining this knowledge with the observation from the Human Protein Atlas that PDILT is possibly expressed in melanoma tissue and that disrupting PDI expression in the ER has therapeutic potential, the expression of PDILT in melanoma should be further investigated to evaluate if it is also facilitating cancer cell survival. This would also open up the possibility for targeting PDILT therapeutically as a potential treatment.

1.13. Thesis Aims

The aims of this thesis are as follows:

- To investigate which structural features are required for PDILT to interact with partner proteins. This will be done by analysing how key mutations impact on PDILTs ability to interact with client proteins.
- To explore the expression of PDILT in melanoma cell lines using a range of experimental approaches including western blotting and immunofluorescence

The hypothesis of this thesis is:

- That solvent exposed cysteine residues are required for PDILT to interact with client proteins.
- That the C terminal tail of PDILT is required for interactions between PDILT and at least some partner or client proteins.
- That testis specific chaperones may be de-repressed in some cell types or disease states.

2. Materials and Methods

2.1 Cell Culture

The human fibrosarcoma HT1080 cells were cultured in Dulbecco's Modified Eagle's Medium (Gibco, ThermoFischer Scientific), which was supplemented with a combination of 2 mM glutamax (Gibco, ThermoFischer Scientific), 100 units/ml penicillin (Gibco, ThermoFischer), 100 µg/ml mM streptomycin (Gibco, ThermoFischer) and 8 % of fetal bovine serum (Sigma). All melanoma cell lines were mycoplasma-free and were kindly donated by Prof Lovat (Institute of Cellular Biology, Newcastle University). These cell lines were A375, WM35, C8161, WM1641, WM164, SKMEL28 and CHL1. All these cell lines were cultured in Dulbecco's Modified Eagle's Medium (Gibco, ThermoFischer Scientific), which was supplemented with a combination of 2 mM glutamax (Gibco, ThermoFischer Scientific), 100 units/ml penicillin (Gibco, ThermoFischer), 100 µg/ml streptomycin (Gibco, ThermoFischer) and 8 % fetal calf serum (Sigma). All cell lines were passaged when 70-90 % confluent using 1 ml 0.05 % trypsin (Gibco, ThermoFischer Scientific) to disrupt the cell monolayer, after which cells were washed three times with 5-10 ml of PBS (Sigma). All cell lines were cultured in an incubator kept at 37˚C and 5 % CO_2. Cell lines were tested for mycoplasma in house by DAPI staining followed by immunofluorescence, examining for contaminating DNA. The cell lines donated from Prof P. Lovat's group were tested for mycoplasma before being gifted to our laboratory.

2.2 Spheroid Culture

Melanoma spheroids were prepared by adding a 5000 melanoma cell suspension in 200 µl of Dulbecco's Modified Eagle's Medium (Gibco, ThermoFischer Scientific) to a 1.5 % noble agar-lined (Sigma) well of a 96 well plate. A 5000 cell suspension was produced by counting a cell suspension solution using a haemocytometer (Improved Neubauer) and then diluted. The resultant cell suspensions were left to incubate for 4, 6 or 8 days at 37˚C and 5 % CO_2, to mimic physiological conditions *in vivo*. Over this incubation time the melanoma cells formed into spheroids. Spheroids were collected from each well, at the relevant time point, using a P1000 pipette and then decanted into a 1.5 ml Eppendorf tube. When the 10 spheroids were harvested, the excess media was then drained from the Eppendorf. The collected spheroids were then either lysed with MNT lysis buffer (20 mM MES, 30 mM Tris, 100 mM NaCl, pH 7.4), for western blotting analysis or prepared for immunofluorescence. Spheroids were prepared for immunofluorescence by adding 4 % paraformaldehyde (VWR Chemicals), diluted in PBS, and allowing the spheroids to fix for 2 hours. Once fixed, the spheroids were

suspended in 5 % agarose (Sigma) and transferred to a 50 ml falcon tube. Once the agarose had solidified it was taken out of the falcon tube and transferred to a histology cassette. The resultant cassette was sent to be imbedded in paraffin by the Histology Department of the Royal Victoria Infirmary, Newcastle.

2.3 Cell Lysis

Cells were lysed either once confluent in a 6 cm dish or 24-48 hours post transfection. 6 cm dishes were washed twice in PBS and then transferred to an ice cooled metal tray coated in tissue soaked with ethanol. 300 µl of lysis buffer (1×Triton x100, 1x MNT (20 mM MES, 30 mM Tris-HCL, 100 mM NaCl, pH 7.4) and 1 µg/ml of a protease inhibitor cocktail comprised of cystatin, leupeptin, antipain, pepstatin A (CLAP)) was applied to the dish and scraped with a cell scraper. The resultant lysate was transferred to a 1.5 ml Eppendorf. SD rat testis tissue was lysed in 1 ml of lysis buffer and subjected to grinding with a pestle and mortar. The resultant lysate was transferred to a 1.5 ml Eppendorf tube. Two frozen melanocyte cell pellets were also kindly donated by Prof Lovat, one with a light pigmentation and one with a dark pigmentation. These pellets were lysed in 300 µl of lysis buffer and then vortexed until all cells were disrupted. All lysates were centrifuged at 16,000 g for 5 minutes at 4˚C. All lysates were stored at -20˚C, after being flash frozen in liquid nitrogen.

2.4 cDNA

The following list of pcDNA 3.1 constructs containing a FLAG tag were kindly donated by K. Araki and K. Nagata, Kyoto University, Japan: WT PDILT; PDILT C135A; PDILT C420A; PDILT C135A/C420A; PDILT DEL498-580; PDILT 520-580; PDILT DEL498-580+C135A/C420A and PDILT DEL520-580+C135A/C420A. The Ero1α -myc pcDNA.3.1 construct has been previously described (Benham et al 2000)

2.5 Antibodies

The PDI polyclonal antibody was produced by immunising rabbits with purified rat PDI, as described (Benham et al. 2000). In western blotting experiments the PDI polyclonal antisera was used at a 1:2000 dilution. The two PDILT antibodies, 2835 and 2836, were produced by immunising rabbits with recombinant PDILT, as partly described (Van Lith et al 2005 and 2007). In western blotting experiments the PDILT antibodies were used at 1:2000, in immunofluorescence experiments they were used at 1:200 and in immunohistochemistry experiments they were diluted 1:250. The anti-myc antibody, 9B11, was used for the

detecting of Ero1α (Cell Signalling Technology, 2279S). In western blotting experiments 9B11 was used at 1:2000, and in immunofluorescence experiments it was used at 1:200. The anti-FLAG antibody (Sigma) was used for the detection of the FLAG-tagged PDILT constructs. In western blotting experiments it was used at 1:1000. The calmegin and calnexin antibodies were produced by and kindly donated by Prof. M Okabe and Prof M. Ikawa (Osaka University, Japan). In western blotting experiments these antibodies were used at 1:2000. A commercial calmegin antibody was also used (abcam, ab172477). When this antibody was used, it has been denoted by the name "CLGN (abcam)". In western blotting experiments ab172477 was used at 1:2000, in immunofluorescence experiments it was used at 1:200 and in immunohistochemistry experiments it was used at 1:250. Finally, an actin antibody was used to assess equal loading between lysates (abcam, ab8224). It was used at 1:10,000 for western blotting.

The secondary antibody donkey anti-rabbit Alexa fluor 594 was used for visualisation in immunofluorescence experiments, used at a 1:1000 concentration. Goat anti-Rabbit Alexa fluor 568 was also used for visualisation in immunofluorescence and immunohistochemistry experiments, used at a 1:1000 and 1:250 respectively. Goat anti-mouse Alexa fluor 488, used at 1:1000. The secondary antibodies SARPO (Swine Anti-Rabbit Peroxidase) and GAMPO (Goat Anti-Mouse Peroxidase; both from Agilent) were used for western blotting detection at 1:3000.

2.6 Bradford Assay

The protein concentration of all samples was determined with a Bradford assay. The Bradford dye (Coomassie Brilliant Blue G-250), when in acidic conditions, converts from its cationic form to its anionic form, becoming blue in the process. This anionic form of the Bradford dye binds to proteins in the lysate subject to analysis, forming a stable interaction. Due to this binding, the concentration of protein in a lysate can be determined by the amount of dye present. The amount of dye can be measured by its absorption spectrum at 595 nm using a spectrophotometer.

Six Bradford standards were produced by the dilution of 1 mg/ml BSA (Sigma) in lysis buffer. The standards were 0, 1, 2, 4, 8 and 10 µg/ml. These BSA standard solutions and lysates were combined with 10 µl 0.1 M HCl, 80 µl ddH_2O and 900 µl Bradford Dye (Biorad). The coomassie dye was first diluted 1:5 in ddH_20. The absorbances of the BSA standard samples

and lysate samples were then measured at 595 nm using a Biophotometer (Eppendorf Biophotometer). The Bradford standards were then plotted on a line of best fit. The lysate samples were compared to the line of best fit to determine their protein concentration.

2.7 SDS-PAGE

Samples were prepared for SDS-PAGE by boiling an equal volume of 2 x Laemmli sample buffer (65.8 mM Tris-HCl, 26.2 % glycerol, 2.1 % SDS and 0.001 % bromophenol blue, pH 6.8) with lysate for 5 min at 95˚C in a heating block. The samples were then centrifuged for 1 min at 16,000 g at room temperature. If samples required reduction 50 mM of DTT was also included in the sample buffer. Either 10 or 15 well SDS-PAGE gels were cast. Ten well SDS-PAGE gels were loaded with a maximum volume of 5 µl of lysate and 15 well SDS-PAGE gels were loaded with a maximum volume of 10 µl of sample lysate.

The resolving gel was comprised of 4.8 ml ddH_20, 2.5 ml 40 % acrylamide, 2.5 ml 1.5 M Tris pH 8.8, 100 µl 10 % SDS, 100 µl 10 % APS and 4 µl TEMED. The stacking gel was comprised of 1.5 ml ddH_20, 250 µl 40 % acrylamide, 250 µl 1.0 M Tris pH 8.8, 20 µl 10 % SDS, 15 µl 10 % APS and 2 µl TEMED. The resolving gel was pipetted into a gel caster (Hoefer) and left to polymerise for 30-45 minutes. Whilst polymerising, the resolving gel was covered with 400-600 µl of ddH_20. Once polymerised, the ddH_20 was removed and the stacking gel was pipetted into the gel caster, with either a 10 or 15 well gel comb inserted prior to polymerisation. The gel was left to polymerise for 5-10 minutes. Following this, the gel(s) was loaded and placed into a gel electrophoresis unit (SE250 Mighty Small II Mini Vertical Electrophoresis Unit, Hoefer), and then filled with running buffer, produced by diluting 10x TGS to 1x TGS in ddH_20 (Biorad - 25 mM Tris base, 190 mM glycine and 0.1 % SDS). 5-10 µg of the sample protein were loaded alongside a prestained protein ladder (Precision Plus, Biorad), to allow identification of protein molecular weights. The sample loaded gel was then electrophoresed at 50 mA for 1-2 hours, using a power pack (Biorad PowerPac 300). The resultant gel was then analysed by western blotting.

2.8 Western Blotting

SDS-PAGE gels were produced, as described in Section 2.6, and then subject to protein transfer. An Immobilon PVDF membrane (Millipore) was primed by incubating the membrane in methanol for 15 seconds. The primed membrane was then stored in transfer buffer (25 mM Tris-Base, 190 mM Glycine and 20 % methanol, pH 9-9.4) until use. The gel

was then prepared for transfer in a cassette. The cassette was prepared by placing the PVDF membrane and gel together, with two filter papers and two sponges either side of this arrangement. The sponges and filter papers were soaked in transfer buffer before placement in the cassette.

Once the sandwich had been assembled in the cassette, the cassette was closed and inserted into the transfer kit (Biorad Mini Trans-Blot Cell), together with an ice-cold cooling unit. The transfer kit was then filled with chilled transfer buffer and run at 150 mA for 120-180 minutes, at room temperature, or run at 30 V overnight, at 4˚C, using power pack (Biorad PowerPac 300). Once transfer was completed, the transfer cassette was disassembled and the membrane was extracted. The membrane was then blocked in a 5 % w/v milk solution (Tesco Instant Dried Skimmed Milk in TBS-T - 10 mM Tris-Base, 70 mM NaCl, 1.75 mM KCl and 0.1 % Tween) overnight, on a rocker at 4˚C.

Following blocking, the membrane was transferred to a 50 ml tube and then washed in TBS-T a total of five times, incubating the membrane for 5 min between washes. The primary antibody was then applied in 1 ml of 2 % milk/TBS-T and the membrane was allowed to incubate for one hour. After this incubation, the membrane was then washed five times in TBS-T. The secondary antibody SARPO (swine anti-rabbit peroxidase) or GAMPO (goat anti-mouse peroxidase) was then applied to the membrane in 1 ml of 2 % milk/TBS-T, and incubated for 1 hour. After this incubation had elapsed, the membrane was then washed for a total of five times in TBS-T.

The membrane was then briefly washed in TBS (10 mM Tris-Base, 140 mM NaCl and 1.75 mM KCl), with the excess liquid removed by dabbing on paper towel, and then the membrane was placed on saran wrap. Next, 500 µl ECL solution (GE Healthcare) was applied to the membrane, to allow for band visualisation by chemiluminescence. The excess ECL was then dabbed off and the membrane placed on new saran wrap. The membrane was then exposed to photographic light sensitive film (ThermoFischer), whilst in a dark room. The film was then developed with an X-ray developer machine (XOMAT).

2.9 Transfection

Transfection was carried out on HT1080 cells, grown to 70-90 % confluency in 6 cm dishes, using Lipofectamine 3000 (Invitrogen).

Cells were prepared for transfection by washing the cells with PBS twice. Two different transfection solutions were prepared and then applied to the cells. The first solution was made with 125 µl of OptiMEM (Gibco, ThermoFischer) and 3.75 or 7.50 µl of Lipofectamine 3000. The second solution was made with 125 µl of OptiMEM, 5 µl of P3000 Enhancer Reagent and either 1 µg or 2 µg of cDNA. Following application of the two transfection solutions to the cells, a further 250 µl of OptiMEM was applied to the cells. The cells were then incubated in a tissue culture incubator at 37˚C and 5 % CO_2. After this hour had elapsed, 1 ml of OptiMEM was applied to the cells. The cells were ready for lysis 24-48 hours later.

2.10 Immunofluorescence of Adherent Cells

Cells were grown on 18 mm coverslips in 6 cm dishes, until they were 70-90 % confluent. The coverslips were then washed twice in PBS. The coverslips were then prepared for immunofluorescence by fixing with 4 % paraformaldehyde, diluted in PBS++ (PBS supplemented with 1 mM $CaCl_2$ and 0.5 mM $MgCl_2$, Sigma). After allowing 15 minutes to fix, the cells were washed twice in PBS++. All free aldehyde groups were quenched via application of 50 mM NH_4CL_2 for 15 minutes. Once this time had elapsed, the coverslips were washed again three times in PBS++. Cells on the coverslips were then permeabilization with 0.1 % Triton-x100, diluted in PBS++. After allowing 10 minutes for the permeabilized to be completed, the coverslips were washed again in PBS++.
Next, 25 µl of primary antibody, at the concentrations described in section 2.5, were applied to the coverslips in a 0.2 % BSA solution, diluted with PBS++. The coverslips were left for 20 minutes and then washed with PBS++ three times.

The relevant secondary antibody was then applied at 1:1000 in 25 µl of 0.2 % BSA solution. The secondary antibodies used in this work were the donkey anti-rabbit Alexa Fluor 594, the mouse monoclonal Alexa Fluor 568 and the goat anti-mouse Alexa Fluor 488 (all Invitrogen, ThermoFischer Scientific). The secondary antibody was incubated with the coverslip for 25 minutes and following this incubation, the coverslips were washed twice in PBS++. The coverslips were incubated with DAPI, diluted to 0.1 ug/ml in PBS++, for 5 minutes.

Following this procedure, the coverslips were briefly washed in ddH_2O to remove excess PBS and then mounted onto microscope slides using vectashield (Vector laboratories).

Immunofluorescence was then imaged using either a Zeiss Apotome or a Zeiss 880 confocal microscope.

2.11 Cell Spheroid Immunofluorescence

Spheroids imbedded in paraffin were produced as described in section 2.2. The paraffin blocks were then mounted onto a microtome (Microm HM 330 Microtome) and cut into 4 µm sections. These sections were mounted onto slides and then baked at 60˚C overnight.

Once adhered to the slides, the spheroid sections were incubated in Histo-Clear (National Diagnostics) for 15 minutes. The slides were then hydrated through a series of alcohols. Each slide spent 3 minutes in 100 %, 95 % and 70 % ethanol. Finally, the spheroid sections were incubated in deionised water for 3 minutes.

The spheroid sections were then subject to antigen retrieval. Sections were heated in a microwave at full power in preheated 1x sodium citrate for 10 minutes. 1x sodium citrate was produced by diluting a 10x sodium citrate stock (74.4 mM anhydrous sodium citrate) 1:10 in ddH_20. The sections were then allowed to rest for one minute and then they were heated again at full power for another 5 minutes in the sodium citrate. Sections were then cooled on the bench for 20 minutes and subsequently permeabilized by incubating the slides in permeabilizing buffer (0.1 % Triton x100, diluted in 1x PBS) on a rocker for 20 minutes. Finally, sections were blocked by incubating the slides in blocking buffer (2 % FBS in PBS with 0.1 % Tween20) for 30 minutes.
Primary antibodies, secondary antibodies and the DAPI nuclear stain were then applied to the sections in the same manner as described in section 2.10.

2.12 Immunohistochemistry Protocol

Six human melanoma tissue samples were kindly donated by Prof. Lovat for examination. Permission to use this tissue was obtained from the national research ethics committee (08/H0906197+5_Lovat). The nature of these tumours is outlined in Table 3. These tumours were sectioned, hydrated, subject to antigen retrieval and stained in a similar manner as described in section 2.11.

3. Results Section – Chapter 1

3.1. Transfection and localisation of PDILT and Ero1α in transfected HT1080 Cells

One of the aims of this thesis was to examine how mutations to key structural elements of PDILT effect its ability to interact with client proteins. An alignment of the PDI and PDILT protein sequences can be seen in Figure 5. The key structural elements of interest are the two cysteines present at position 135 and 420 and also the C-terminal extension. In order to examine the role of these free cysteines, a series of mutations have already been performed and several PDILT constructs have been generated. These were either generated in-house or kindly donated to our laboratory by Dr. Araki and Prof. Nagata, Kyoto University, Japan. A summary of the PDILT mutants generated for this study can be found in Figure 6. In summary, cysteines 135 and 420 in PDILT have been replaced with alanine. The C terminal tail domain of PDILT was mutated, with two separate deletions at different points along the tail. The final set of constructs combines the cysteine substitution and C-terminal tail deletion. These constructs required further evaluation in cell lines. Thus, a series of transfection experiments were performed using HT1080 cells to establish their suitability for the analysis of these PDILT cDNA constructs and for the comparison of FLAG-tagged and myc-tagged PDILT proteins.

HT1080 cells were grown to confluence in 6cm dishes and then transfected with either PDILT wt cDNA, Ero1α-myc cDNA, or mock transfected using Lipofectamine 3000 as a transfection reagent. Twenty-four hours after transfection the transfected HT1080 cells were lysed using MNT lysis buffer. The resulting lysates were then centrifuged at 16000 g to separate the nuclear components from the cellular components. Rat testis was also lysed with MNT lysis buffer and diluted 1:10 to act as a positive control. These samples were then loaded onto an SDS-PAGE gel and run under reducing and non-reducing conditions and blotted with a PDILT antibody (2835), a PDI antibody and an anti-Myc antibody (9B11), as the transfected Ero1α has a myc tag. The Figure 7A demonstrates that the HT1080 cells were successfully transfected with PDILT, as a clear band at ~ 77 kD can be seen. This correlates with a band of a similar molecular weight in the positive control, the rat testis lysate. The PDI blot in the Figure 7B showed a single band in all lysates at around 55 kD, which would be expected for this universally expressed protein. The Figure 7C demonstrates that the transfection of Ero1α was also successful, as only the Ero1α transfected lysate had a band present at around 60 kD, which is expected given the molecular weight of the protein. These western

blot results taken together show that HT1080 cells are suitable hosts for transfection as they are able to express transfected proteins at a level that can be detected by western blotting. Equal protein loading of the lanes was ensured with an actin blot (not shown).

```
PDILT : MDLLWMPLLLVAACVSAVHSSPEVNAGVSSIHITKPVHILEERSLLVLTPAGLTQMLNQT 60
PDI   : --MLRRALL----CLAVA-------------ALVRADAPEEEDHVLVLRKSNFAEALAAH 41
          :*   **    *::..              :.:     **  :***  :.::: *

PDILT : RFLMVLFHNPSSKQSRNLAEELGKAVEIMGKGKNGIGFGKVDITIEKELQQEFGITKAPE 120
PDI   : KYLLVEFYAPWCGHCKALAPEYAKAAGKLKAEGSEIRLAKVDATEESDLAQQYGVRGYPT 101
        ::*:* *: * . :.: ** * .**.  :    . * :.*** * *.:* *::*:   *

PDILT : LKLFFEGNRSEPISCKGVVESAALVVWLRRQISQKAFLFNSSEQVAEFVISRPLVIVGFF 180
PDI   : IKFFRNGDTASPKEYTAGREADDIVNWLKKRTGPAATTLPDGAAAESLVESSEVAVIGFF 161
        :*:* :*: :.* . ..  *:  :* **::: .  *  : ..  . .:* *  :.::***

PDILT : QDLEEEVAELFYDVIKDFPELTFGVITIGNVIGRFHVTLDSVLVFKKGKIVNRQKLINDS 240
PDI   : KDVESDSAKQFLQAAEAIDDIPFGITSNSDVFSKYQLDKDGVVLFKKFDEG--RNNFEGE 219
        :*:*.: *: * :. : : :: **: : .:*:.::::  *.*::*** .    :: ::..

PDILT : TNKQELNRVIKQHLTDFVIEYNTENKDLISELHIMSHMLLFVSKSSESYGIIIQHYKLAS 300
PDI   : VTKENLLDFIKHNQLPLVIEFTEQTAPKIFGGEIKTHILLFLPKSVSDYDGKLSNFKTAA 279
        ..*::*  .**::   :***:. :.   *   .* :*:***: ** ..*.  :.::* *:

PDILT : KEFQNKILFILVDADEPRNGRVFKYFRVTEVDIPSVQILNLSSD-ARYKMPSDDITYESL 359
PDI   : ESFKGKILFIFIDSDHTDNQRILEFFGLKKEECPAVRLITLEEEMTKYKPESEELTAERI 339
        :.*:.*****::*:*.  * *::::* :.: : *:*:::.*..: ::**  *:::* * :

PDILT : KKFGRSFLSKNATKHQSSEEIPKYWDQGLVKQLVGKNFNVVVFDKEKDVFVMFYAPWSKK 419
PDI   : TEFCHRFLEGKIKPHLMSQELPEDWDKQPVKVLVGKNFEDVAFDEKKNVFVEFYAPWCGH 399
        .:* : **. : . *  *:*:*: **:  ** ******: *.**::*:*** *****. :

PDILT : CKMLFPLLEELGRKYQNHSTIIIAKIDVTANDIQLMYLDRYPFFRLFPSGSQQ-AVLYKG 478
PDI   : CKQLAPIWDKLGETYKDHENIVIAKMDSTANEVEAVKVHSFPTLKFFPASADRTVIDYNG 459
        ** * *: ::**..*::*..*:***:* ***::: : :. :* :::**:.::: .: *:*

PDILT : EHTLKGFSDFLESHIKTKIEDEDELLSVEQNEVIEEEVLAEEKEVPMMRKGLPEQQSPEL 538
PDI   : ERTLDGFKKFLESGGQDGAGDDDDLEDLEEAEEPDME---EDDDQKAVKDEL-------- 508
        *:**.**..****  :    *:*:* .:*: *  : *   *:.:   ::. *

PDILT : ENMTKYVSKLEEPAGKKKTSEEVVVVVAKPKGPPVQKKKPKVKEEL 584
PDI   : ---------------------------------------------
```

Figure 5: The Sequence of PDILT compared to PDI. The protein sequence of PDILT compared to the protein sequence of PDI, generated by UniProt.

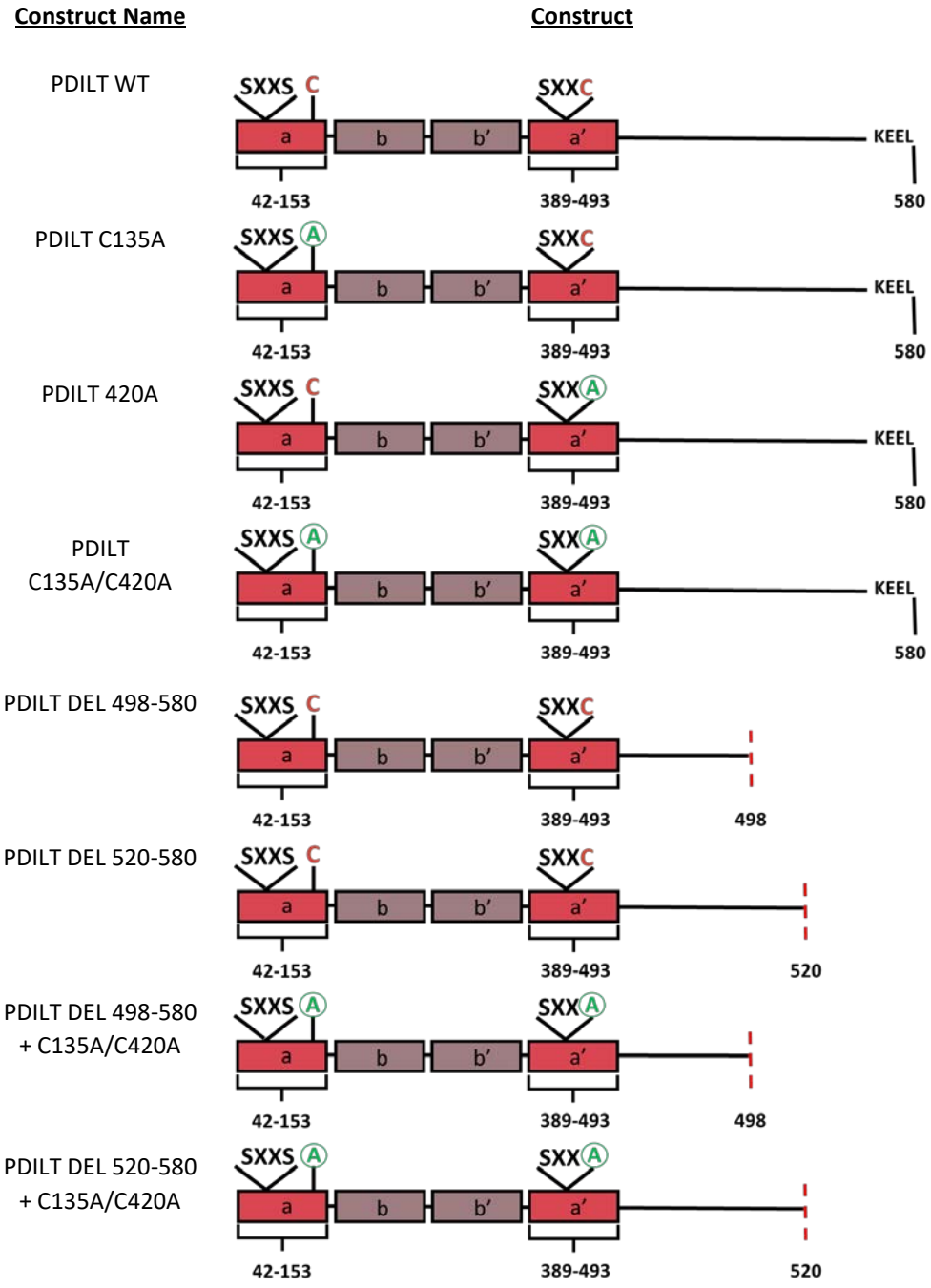

Figure 6: The Mutant PDILT Constructs. Diagrammatic representation of mutagenesis of the PDILT constructs. All constructs also contained a FLAG tag upstream of the KEEL ER retention sequence.

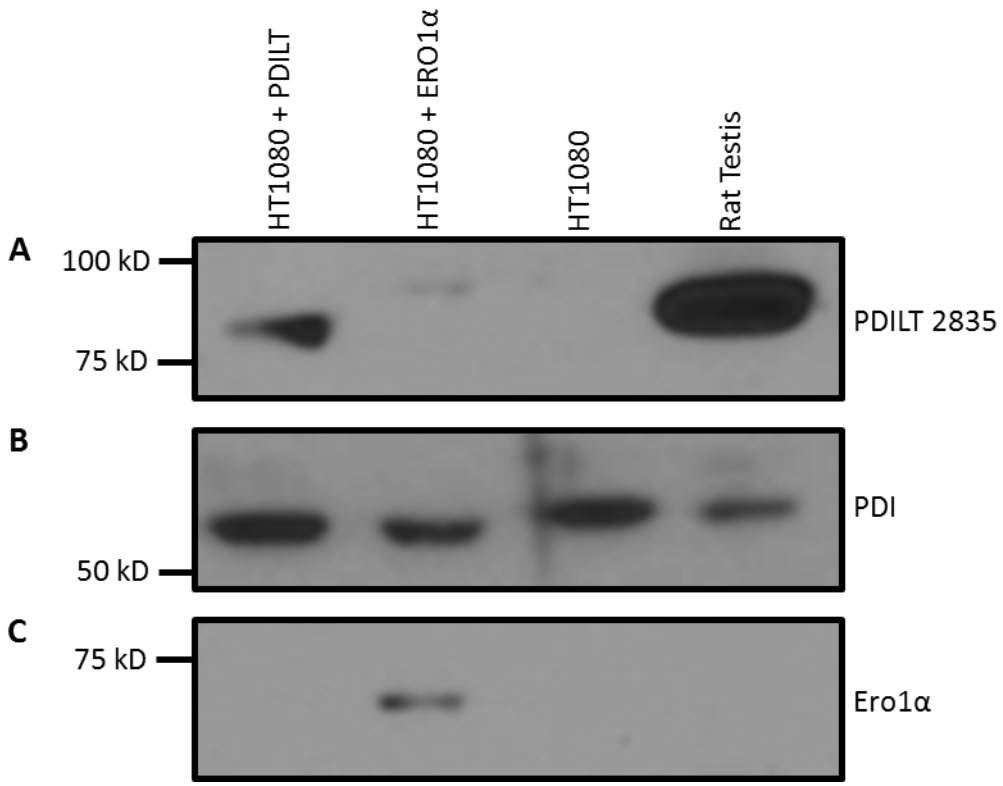

Figure 7: Western Blot of HT1080 Cell Lysates Transfected with PDILT and Ero1α. The transfected HT1080 cell lysates were run on an SDS-PAGE gel, transferred to PVDF membranes and blotted with a PDILT 2835 antibody (**A**), PDI antibody (**B**) and an anti-Myc antibody (**C**). An untransfected HT1080 lysate acted as a negative control and a rat testis lysate acted as a positive control for PDILT expression. Only the HT1080 + PDILT lysate and the rat testis lysate showed bands around the 75 kD, confirming successful transfection. Only the HT1080 + Ero1α lysate showed a band around the 55 kD, confirming the transfection of Ero1α into HT1080 cells was successful. All lysates showed expression of PDI when blotting with the PDI antibody.

To further test the localisation of expression of the transfected proteins, a series of immunofluorescence experiments were carried out on HT1080 cells transfected with either PDILT or Ero1α. HT1080 cells were grown on cover slips and then either mock transfected or transfected with PDILT or Ero1α. The cells were then stained with the primary antibody for either PDILT or anti-myc (to identify Ero1α), then the cells were incubated with the secondary antibody conjugated to Alexa fluor 594. Cells were also costained with DAPI for identification of the nuclei. Figure 8A and Figure 8B show that the HT1080 cells successfully transfected with PDILT had perinuclear staining that was consistent with localisation to the ER, which would be expected for PDILT. Staining of Ero1α transfected cells was less clear. Figure 8C and Figure 8D had some speckled staining throughout the cells but most cells demonstrated a stronger intensity of staining around the nucleus, suggesting that Ero1α is expressed and is localised to the ER as anticipated. However, the poor transfection efficiency observed from the images and the speckled staining seen in the mock transfected images (Figure 8E and Figure 8F) suggests that the transfection procedure was sub-optimal.

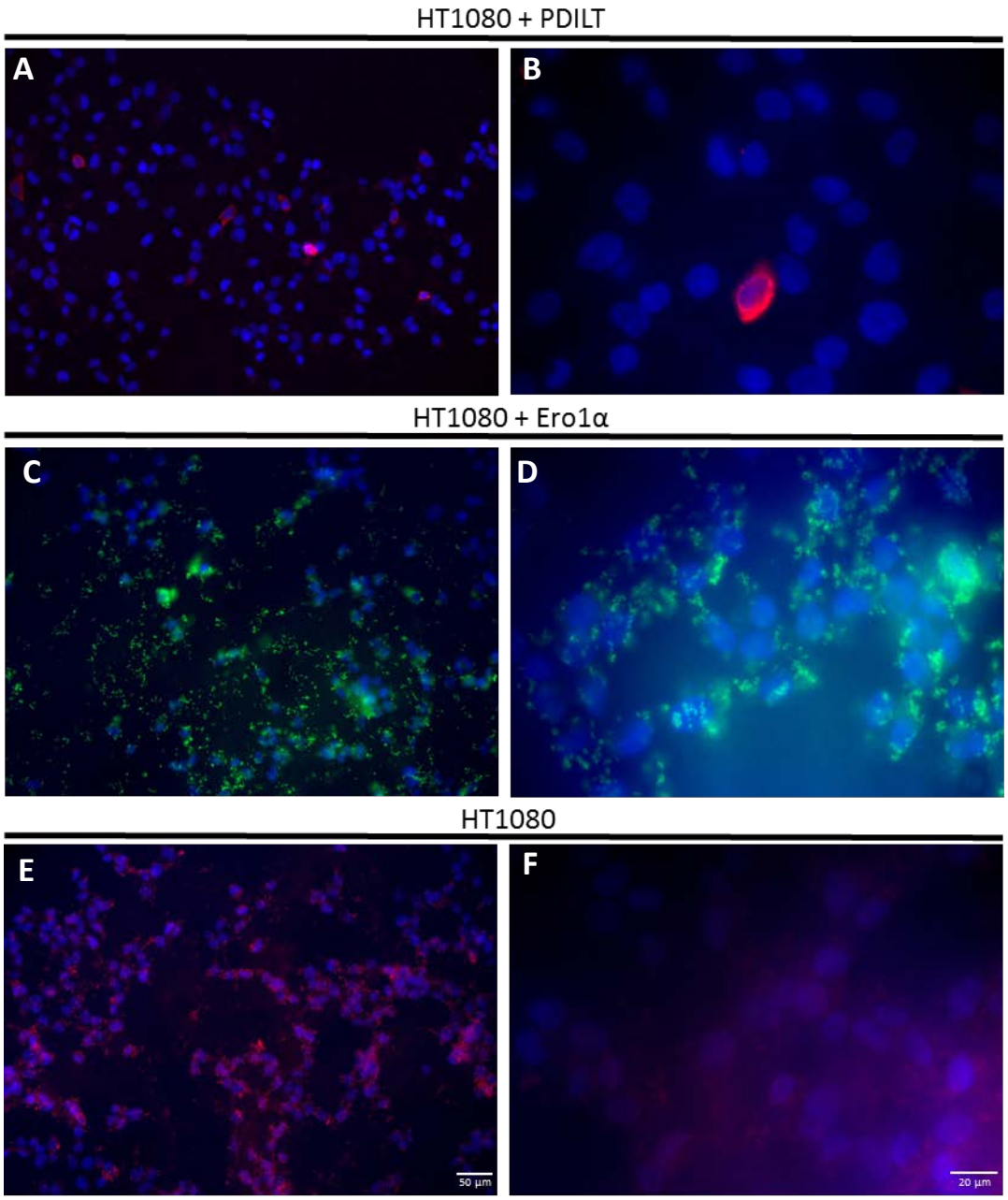

Figure 8: Immunofluorescence of HT1080 Cells Transfected with PDILT and Ero1α. HT1080 cells were transfected with PDILT (**A**-**B**) or with Ero1α (**C**-**D**) or mock transfected (**E**-**F**). PDILT was detected with a PDILT antibody (2835), panels **A** and **B**. Ero1α was detected with an Anti-myc antibody (9B11), panels **C** and **D**. No primary antibody was applied to panel **E** and **F**. The speckled staining seen in **E** and **F** can be used to rule out similar staining in **A**-**D** as PDILT or Ero1α staining. All cells were co-stained with DAPI. When the HT1080 cells transfected with PDILT were stained with the PDILT 2835 antibody, the cells showed perinuclear staining, confirming the expected localisation of PDILT. When the HT1080 cells transfected with Ero1α were stained with the Ero1α antibody, some cells had perinuclear staining, but punctate staining can also be seen in the cells. Images **A C E** were taken at a ×20 magnification with a Zeiss Apotome and images **B D F** were taken at a ×63 magnification on the same microscope. The scale for the 20x magnification images is 50µm and the scale for the x63 magnification images is 20µm.

Given the results from the previous experiments, there was a desire to improve transfection efficiency, thus optimisation of transfection experiments were carried out. HT1080 cells were grown on coverslips and transfected with Ero1α. Different ratios of cDNA and lipofectamine were used to see which conditions improved transfection efficiency. The cDNA was either applied to the cells at 1 µg or 2.50 µg together with either 3.75 µl or 7.50 µl Lipofectamine. Post transfection, the coverslips were incubated with an anti-Myc antibody (9B11) and the secondary antibody coupled to Alexa fluor 594. The coverslips were also incubated with DAPI to stain cell nuclei for cell identification. Transfection efficiency was measured by counting stained cells within a representative field. Regardless of lipofectamine volume, when only 1µg of cDNA was used the transfection efficiency was still poor, as transfection efficiency was roughly 2 % when 3.75 µl of Lipofectamine was used (Figure 9A) and also roughly 2 % when 7.50 µl of Lipofectamine was used (Figure 9B). However, when the cDNA amount was increased to 2.50 µg there was an observable improvement in transfection efficiency. Transfection efficiency improved when this concentration of cDNA was combined with 3.75 µl of Lipofectamine, as it increased to roughly 6 % (Figure 9C). When 7.50 µl of Lipofectamine was used the transfection efficiency was also increased to around 6 % (Figure 9D). While there was a notable difference between 1 µg of cDNA and 2 µg of cDNA, there was not a dramatic difference between the two Lipofectamine volumes. This was still a suboptimal transfection efficiency however and although further optimisation could have been performed, it was decided to use 2 µg of cDNA and 3.75 µl of Lipofectamine 3000 in future experiments.

3.2. Examination of the Impact of Structural Mutations on PDILT Client Interactions

In order to study how the tail domain of PDILT contributes to its function, PDILT constructs with a FLAG tag upstream of the KDEL ER retention sequence were used. The cysteine at position 135 was replaced with alanine (PDILT C135A) and the cysteine at position 420 was also substituted with alanine (PDILT C420A). Both cysteines were also substituted for alanine in a double mutant (PDILT C135A/C420A). The large C terminal extension was deleted at positon 498 (PDILT DEL 498-580) and position 520 (PDILT DEL 520-580). The two tail mutants were combined with the double cysteine mutant (PDILT DEL 498-580+C135A/C420A and PDILT DEL 520-580+C135A/C420A). A wild type FLAG tagged PDILT (PDILT WT) was also used. A list of all PDILT constructs used is shown in Figure 6.

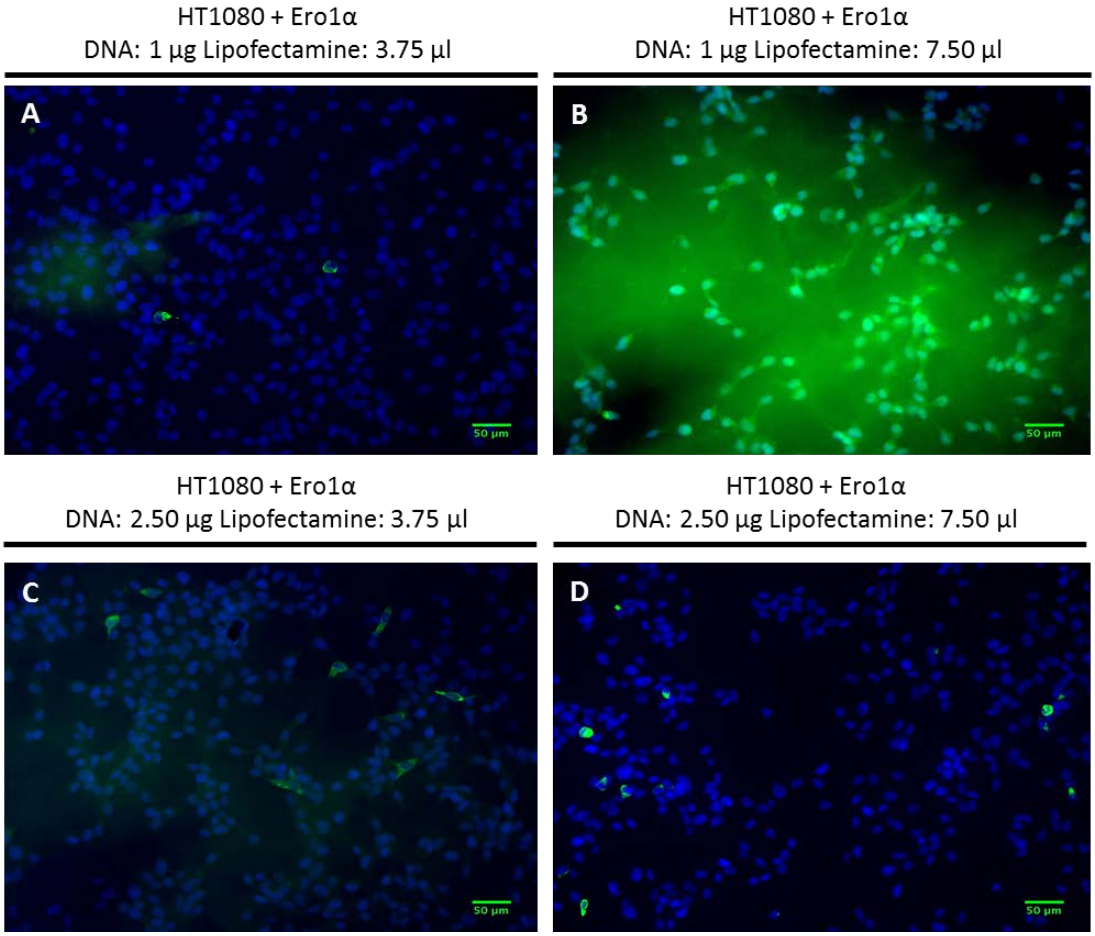

Figure 9: Initial Optimisation of Transfection of HT1080 cells. Different ratios of Ero1α DNA and Lipofectamine 3000 were used to establish transfection efficiency. Ero1α was detected using an Anti-myc antibody (9B11), the secondary antibody Alexa Fluor 488 and also costained with DAPI. (**A**) 1 µg cDNA and 3.75 µl lipofectamine (**B**) 1 µg cDNA and 7.50 µl lipofectamine (**C**) 2.5 µg cDNA and 3.75 µl lipofectamine and(**D**) 2.5 µg DNA and 7.50 µl Lipofectamine, In each case, a relatively low transfection efficiency was observed, but transfected cells (green) demonstrated perinuclear ER staining as expected. The scale for the 20x magnification images is 50µm. The green haze in **B** is due to background staining of the secondary antibody.

The effects on PDILT of substituting position 135 and 240 cysteines for alanine has previously been examined by van Lith et al. 2004. Those experiments were carried out on constructs expressing myc tagged PDILT, unlike these constructs, which express FLAG tagged PDILT. Thus, one of the aims of this thesis was to compare the expression and behaviour of the FLAG-tagged PDILT with the myc-tagged PDILT proteins.

In order to examine what effect these mutations had, the expression of PDILT and PDILTs ability to interact with clients was assessed through a series of western blotting experiments. HT1080 cells were grown to confluency in 6 cm dishes and then transfected with the PDILT constructs. The transfected HT1080 cells were then lysed and run on an SDS-PAGE gel under reducing and non-reducing conditions and blotted with a PDILT antibody (2835). The transfected HT1080 lysates were compared against a mock transfected HT1080 cell lysate as a negative control and a rat testis lysate as a positive control. Figure 10 demonstrates the effects of each mutation on the ability of PDILT to bind with client proteins. The HT1080 lysate transfected with the wild type PDILT demonstrated the expected result, Figure 10 Lane 1, with a high weight molecular series of bands forming at 250 kD, which is consistent with published PDILT complex formation with disulfide-bonded client proteins (van Lith et al. 2007). PDILT C135A showed some loss of the high molecular weight banding pattern under non-reducing conditions (Figure 10 Lane 2) with some complexes visible at a slightly lower molecular weight. This suggests that PDILT C135A is able to form some interactions with client proteins, but not the full range as the wild type PDILT. A similar observation was seen with PDILT C420A, Figure 10 Lane 3, with a different high molecular weight band being observed at a lower molecular weight than PDILT WT, again demonstrating that the loss of a single cysteine facilitates some client interactions. When both cysteine mutations were combined, the PDILT C135A/C420A protein completely lost high molecular weight band formation, Figure 10 Lane 4, suggesting that both cysteines were essential for the ability to interact with client proteins in a disulfide-dependent manner. These results were consistent with those observed for PDILT-myc tagged mutants (van Lith et al 2010), demonstrating that differences in the pre-KDEL tag do not influence the binding profile of PDILT.

Removal of the C terminal extension of PDILT (whilst retaining the KDEL) had a different effect on protein-protein interactions. The C terminal deletion at position 489, PDILT DEL 498-580, caused an increase in complex formation over the 150 kD range, Figure 10 Lane 5, with a similar effect seen when the C terminal section was deleted at position 520 (PDILT

DEL 520-580), Figure 10 Lane 6. This banding pattern suggests that PDILT is interacting either with a greater number of client proteins or with higher affinity to the same client proteins when the C terminal extension is removed. When the tail and cysteine mutations were combined, there was a complete absence of any high molecular weight bands (for both PDILT DEL 498-580+C135A/C420A and PDILT DEL 520-580+C135A/C420A), suggesting a complete loss of client interactions, Figure 10 Lane 7 and 8. This result suggests that the C135 and C420 residues are the primary determinants of disulfide-dependent client interaction, but that the tail domain can control the magnitude of client access.

Observation of the reducing gel of these samples (Figure 10B) demonstrated that the interactions observed under non-reducing conditions were disulfide dependent, as the higher molecular weight complexes were dispersed upon reduction with DTT. The monomer band for PDILT+PDILT DEL 498-580+CI35A/C420A ran at a slightly higher molecular weight than expected, but the other monomers of the different PDILT mutants could be detected at the expected molecular weight in the reducing gel. The control actin blot (Figure 10C) shows a reasonable level of protein loading.

In order to confirm that the proteins detected were not cross-reacting with the PDILT antisera, a repeat of the western blot experiment was performed on the same lysates, blotting back with an anti-FLAG antibody, Figure 11A and B. The same overall pattern of PDILT monomer migration and disulfide-dependent client binding was seen as when the PDILT 2835 antibody was used. As a control, the lysates were probed for the expression of actin which confirmed approximately equal loading in the lanes (Figure 11C).

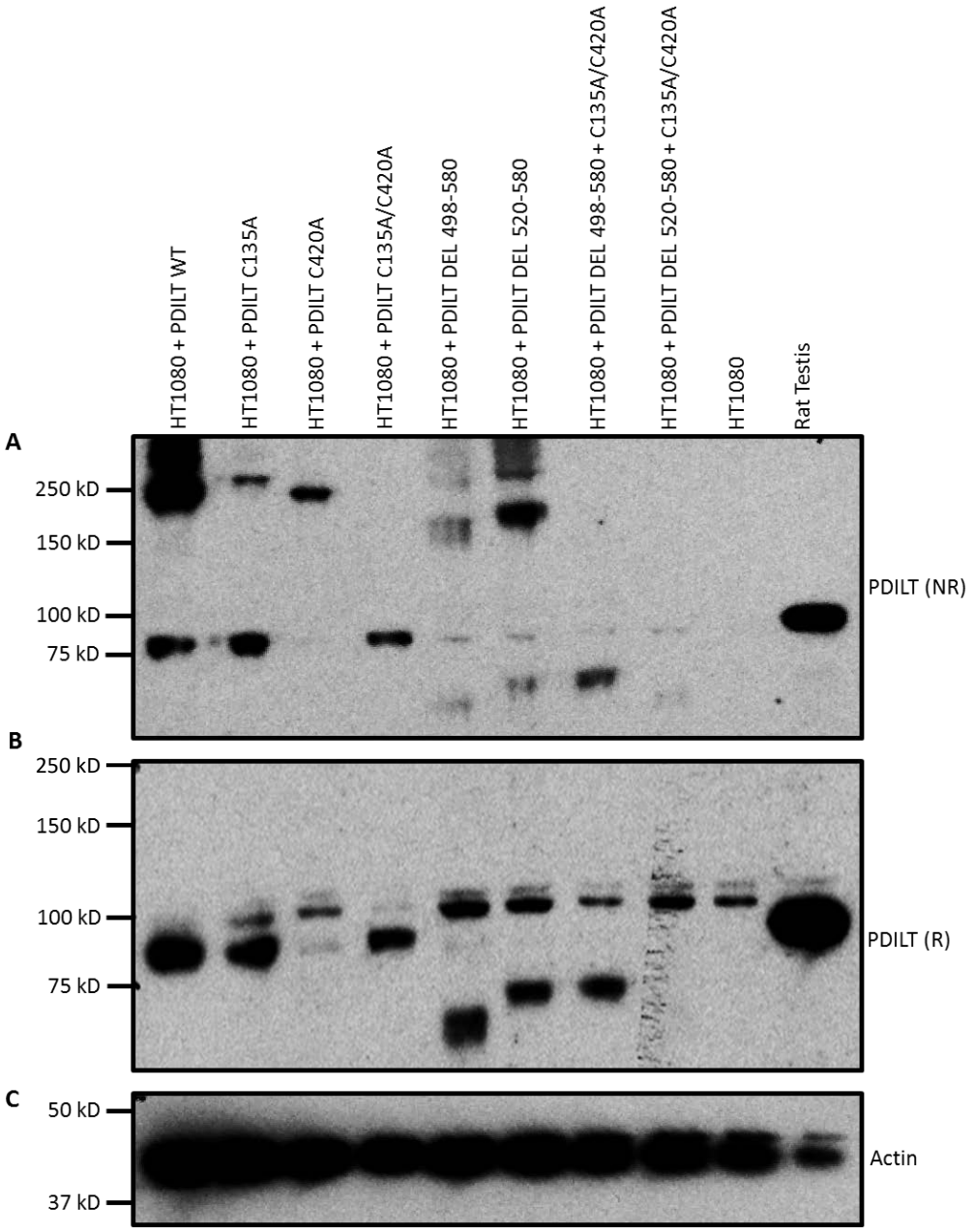

Figure 10: Western blot of HT1080 lysates transfected with PDILT mutants using a PDILT Antibody. The different PDILT constructs listed in Table 1 were transfected into HT1080 cells and lysates were run on SDS-PAGE under non-reducing conditions (NR) (**A**) and reducing conditions (R) (**B**) and blotted with the PDILT 2835 antibody. Actin was used as a loading control (**C**). Under non-reducing conditions, WT PDILT formed a high molecular weight band at 250 kD, confirming PDILT complex formation (Lane 1). PDILT C135A and C420A lost some client interactions (Lanes 2 and 3). PDILT C135A+C420A completely lost high molecular weight bands, suggesting this mutant was unable to interact with disulphide-dependent client proteins (Lane 4). Both PDILT DEL 498-580 and PDILT DEL 520-580 increased the number of client protein interactions (Lane 5 and 6). When both mutations were combined in PDILT DEL 498-580+C135A/C420A and PDILT DEL 520-580+C135A/C420A, there was complete abolishment of high molecular weight bands (Lane 7 and 8). PDILT monomers were confirmed under reducing conditions. The actin antibody confirmed a reasonable level of protein loading.

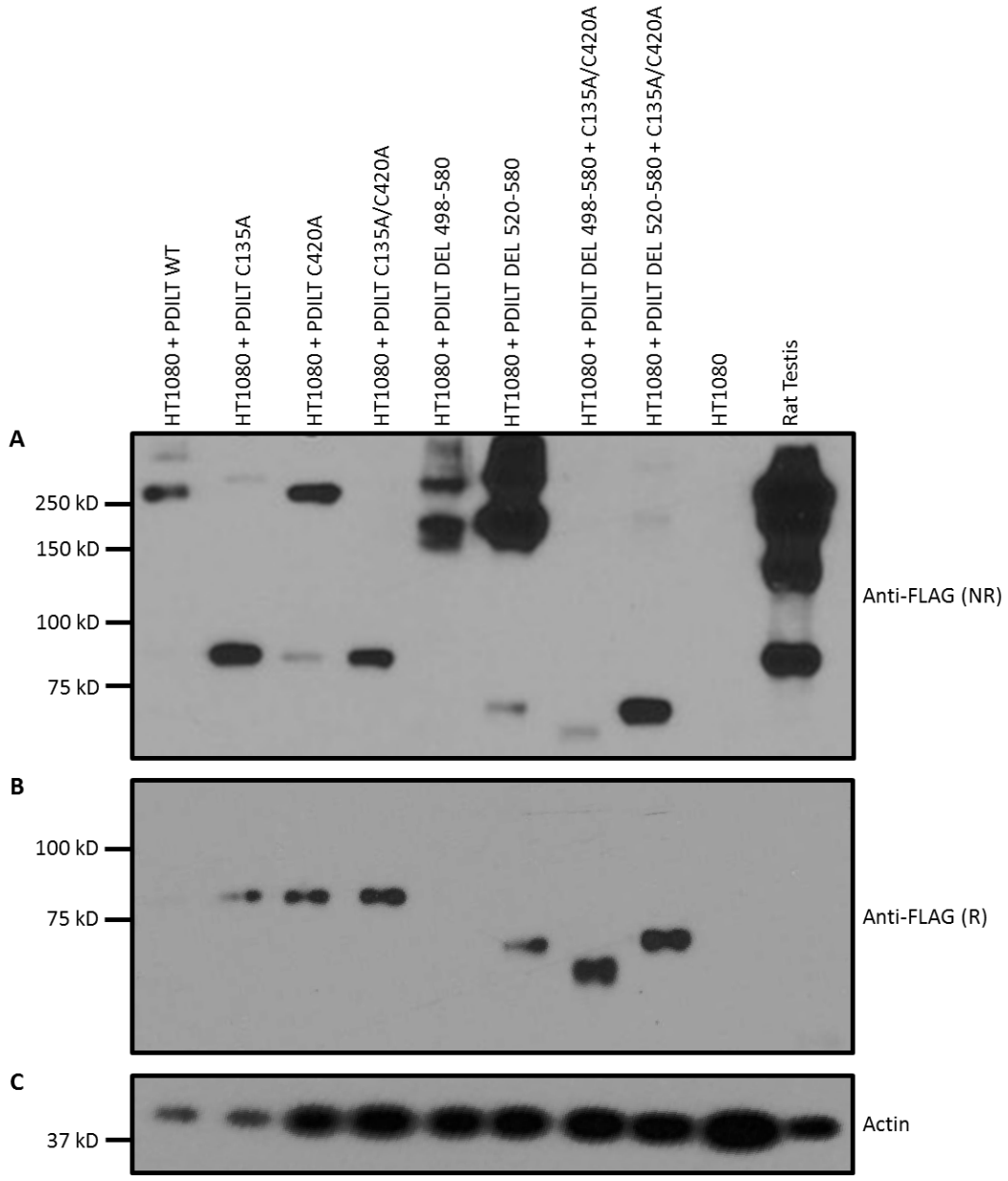

Figure 11: Western blot of HT1080 lysates transfected with PDILT mutants using an Anti-FLAG Antibody. The different PDILT constructs listed in Table 1 were transfected into HT1080 cells and then analysed on an SDS-PAGE by western blotting under non-reducing (NR) conditions (**A**) and reducing (R) conditions (**B**) and blotted with an Anti-FLAG antibody. In the non-reducing blot, WT PDILT formed a range of high molecular weight bands, as seen in Figure 4 (Lane 1). PDILT C135A and C420A both showed a similar loss of client interactions (Lanes 2 and 3) and PDILT C135A+C420A had a total loss of any high molecular weight bands (Lane 4). Both PDILT DEL 498-580 and PDILT DEL 520-580 also showed similar banding to Figure 4, as both had an increase in the number of client protein interactions (Lane 5 and 6). PDILT DEL 498-580+C135A/C420A and PDILT DEL 520-580+C135A/C420A both had a complete loss of high molecular weight bands, again, comparable to Figure 4 (Lane 7 and 8). In the reducing blot, the monomer bands for PDILT WT mutant and the PDILT DEL 498-580 were absent. The actin blot (**C**) confirms a reasonable level of protein loading.

Having established that the PDILT cysteine and tail mutants had different client binding profiles, an experiment was performed to investigate the subcellular localisation of each of the PDILT mutant proteins. HT1080 cells were grown on coverslips, fixed, permeabilized and subjected to immunofluorescence. Each of the coverslips were incubated with the primary antibody PDILT 2835 and the secondary antibody labelled with Alexa fluor 594. Cells were also counterstained with DAPI to allow cell identification. All the transfected HT1080 cells showed strong perinuclear staining consistent with ER localisation, which indicates that all the PDILT variants were successfully targeted to the ER, Figure 12 and 13. The HT1080 cells transfected with PDILT DEL 520-850+C135A/C420A showed some punctate staining, suggesting that some of the PDILT mutant proteins may reside in ER derived vesicles, or are being trafficked for degradation via the lysosomal pathway. This would be consistent with some of the western blotting data in Figure 11, showing that the monomer bands for PDILT WT and PDILT DEL 498-580 were of lower staining intensity in the reducing western blot. However, other explanations could also explain the absence of the monomer bands and the immunofluorescence experiments would need to be repeated, for example using an independent cell line for transfection and with co-labelling of both ER and endosomal-lysosomal markers. Further experimental analysis will be required to understand whether overexpression of PDILT leads to punctate formation, whether a subset of mutant PDILT proteins is prone to misfolding, or whether PDILT is able to access post-ER compartments under physiological conditions.

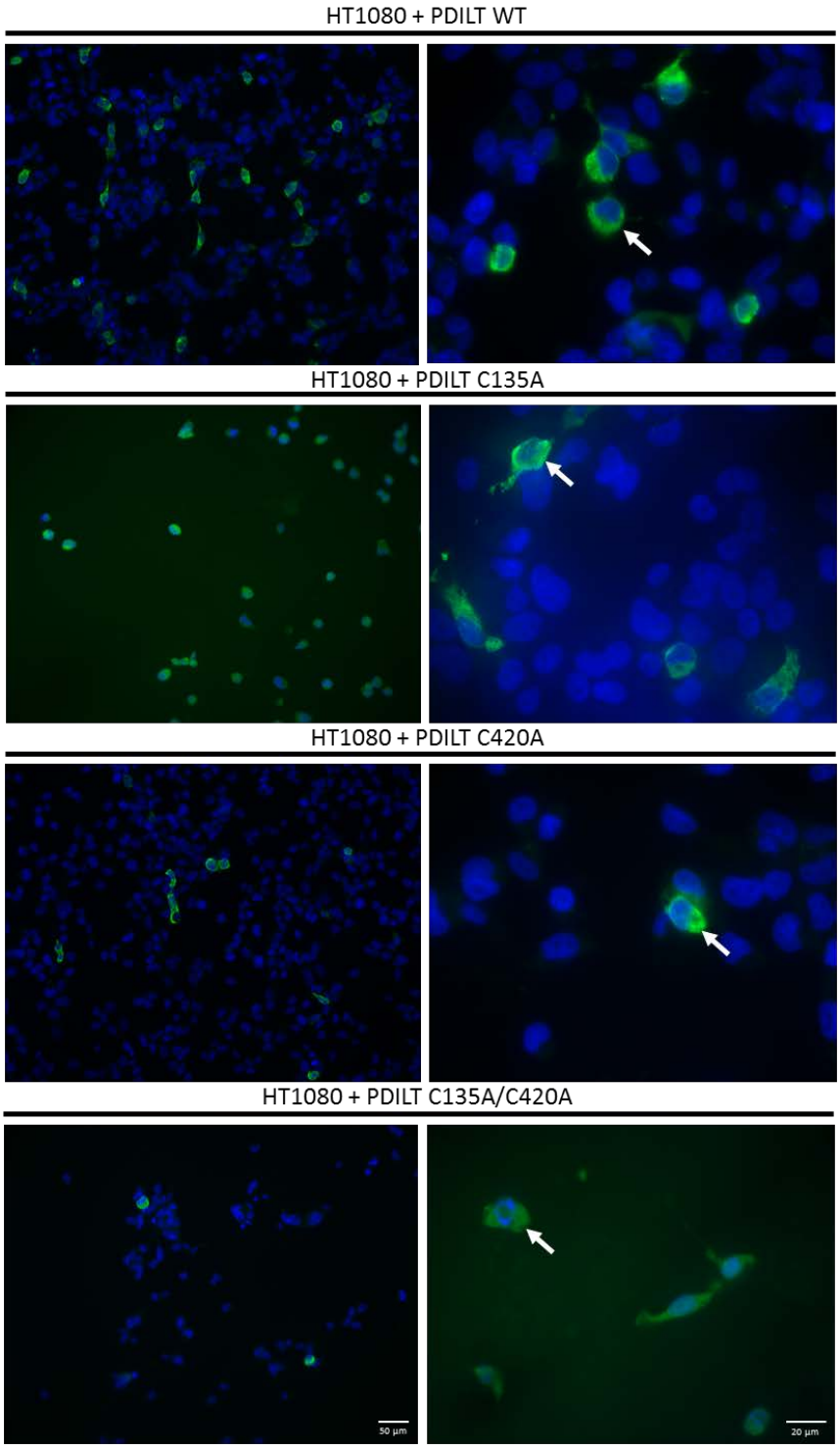

Figure 12: Immunofluorescence of HT1080 Cells Transfected with PDILT mutants. The initial four PDILT constructs listed in Table 1 were transfected into HT1080 cells and the cell prepared for immunofluorescence. The transfected cells were fixed with formaldehyde and then permeabilized with 0.1 % Triton x100. The PDILT mutants were then visualised with a PDILT antibody (2835) and the secondary antibody Alexa Fluor 594. All cells were costained with DAPI. Cells were imaged at ×20 magnification and at ×63 magnification with a Zeiss Apotome. All PDILT mutant proteins localised to a perinuclear region, consistent with the ER. White arrows indicate positive expression. The scale for the 20x magnification images is 50µm and the scale for the x63 magnification images is 20µm.

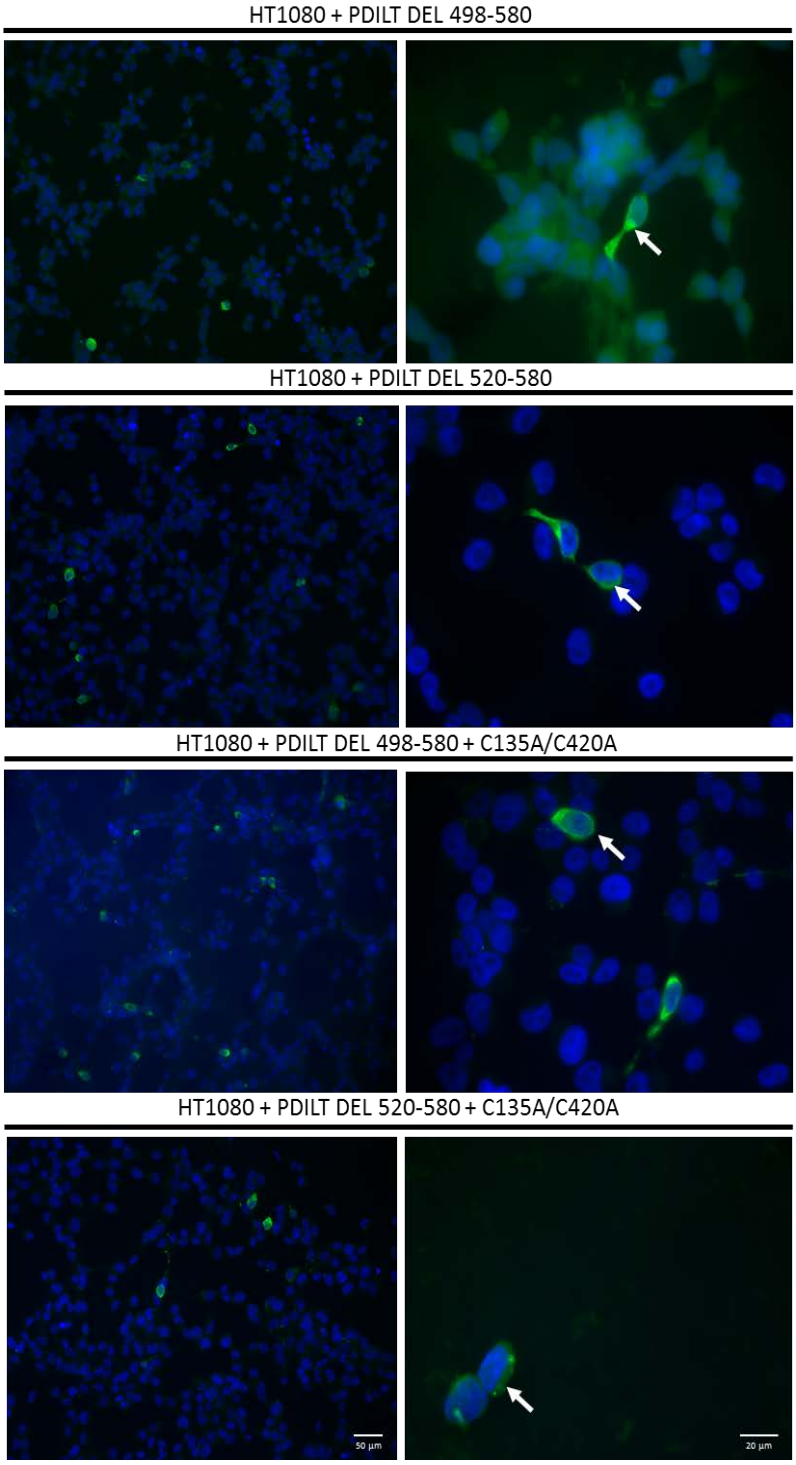

Figure 13: Immunofluorescence of HT1080 Cells Transfected with PDILT mutants. The last four PDILT constructs listed in Table 1 were transfected into HT1080 cells and the cell prepared for immunofluorescence. The transfected cells were fixed with formaldehyde and then permeabilized with 0.1 % Triton x100. The PDILT mutants were then visualised with a PDILT antibody (2835) and the secondary antibody Alexa Fluor 594. All cells were costained with DAPI. Cells were imaged at ×20 magnification and at ×63 magnification with a Zeiss Apotome. All PDILT mutant proteins localised to a perinuclear region, consistent with the ER. White arrows indicate positive expression. The scale for the 20x magnification images is 50µm and the scale for the x63 magnification images is 20µm.

4. Results Section – Chapter 2

4.1. Analysis of Melanoma Cell Lines for Testis Specific ER Protein Expression

To examine the possibility that PDILT might be expressed in melanoma, we decided to test a variety of melanoma cell lines for PDILT expression and other testis specific ER proteins. The six melanoma cell lines were A375, WM35, C8161, WM1361, WM164 and SKMEL28 (kindly provided by Prof Penny Lovat (Dermatological Sciences at Newcastle University). These cell lines were chosen due to their different mutational states in BRAF and NRAS. The mutations present in each of the cell lines are summarised in Table 2.

Initially, the A375, WM35 and the C8161 cell lines were grown in 6 cm cell dishes and lysed with MNT lysis buffer. The resultant lysates were run on an SDS-PAGE gel, transferred to PVDF membranes and blotted with a PDILT antibody (2835) and an actin antibody (Figure 14). Interestingly, the C8161 cell lysate returned a positive result, with a band forming around the 77 kD mark, which is consistent with the correct molecular weight of PDILT and also matches the weight of the band produced by the rat testis control. This suggests that PDILT was expressed in the C8161 cell line but given that this was shown with a single PDILT antibody, another series of experiments were undertaken. All six melanoma cell lines were analysed for PDILT expression with two antibodies and for expression of other testis specific ER proteins.

To test if the observed PDILT expression in C8161 cells was reproducible, each of the cell lines were grown in 6 cm cell dishes and lysed with MNT lysis buffer. The resultant lysates were run on an SDS-PAGE gel and transferred to PVDF membranes which were blotted with two different PDILT antibodies (2835 and 2836), a CLGN antibody, a CNX antibody and an actin antibody. Calmegin was analysed because it is a testis specific ER protein and it is known that testis-specific proteins can be derepressed in melanoma (so-called testis-tumor antigens) (Caballero and Chen 2011). Calnexin was analysed as a positive control because it is a ubiquitously expressed ER protein. All the melanoma cell lysates were compared against a rat testis lysate, which acted as a positive control for testis-specific protein expression. Figure 15A and Figure 15B showed that none of the melanoma cell lysates were positive for PDILT, including C8161. Neither the PDILT 2835 nor the PDILT 2836 antibody revealed a band around the 75 kD mark, which is the molecular weight of PDILT. This conflicts with the

positive result shown in Figure 14. This could be explained by the difference in passage number between the cells lysed. PDILT was evident in the C8161 cell line when cells were lysed at a low passage, at passage 10 (Figure 14), but the C8161 cells appeared to lack expression at a higher passage number, at passage 27 (Figure 15). Figure 15C demonstrates that CLGN was expressed in the C8161 lysate, with the molecular weight of the resultant band, around 100 kD, matching that of the band in the positive control. This suggested that calmegin is expressed in the C8161 cell line. Calnexin was expressed in all of the melanoma cell lines, Figure 15D, as shown by a band around the 80 kD mark, which corresponds with a similar-sized band in the positive control. This was expected given the ubiquitous expression of CNX in all cells. Both the rat testis lysate and the WM35 lysates had doublet CNX bands, one at ~ 90 kD and the other at ~ 80 kD, which was unexpected. This doublet may represent two distinct populations of CNX, which have different post translational modifications. The actin blot in Figure 15E demonstrates that the lysates were approximately equally loaded and transferred.

Table 2: Melanoma Cell Line *The BRAF and NRAS mutation status of the cell lines is provided below.*		
Cell Line	**BRAF**	**NRAS**
A375	V600E	wt
WM35	V599I	wt
C8161	wt	wt
WM1361	wt	Q61R
WM164	V600E	wt
SKMEL28	V600E	wt
CHL1	wt	wt

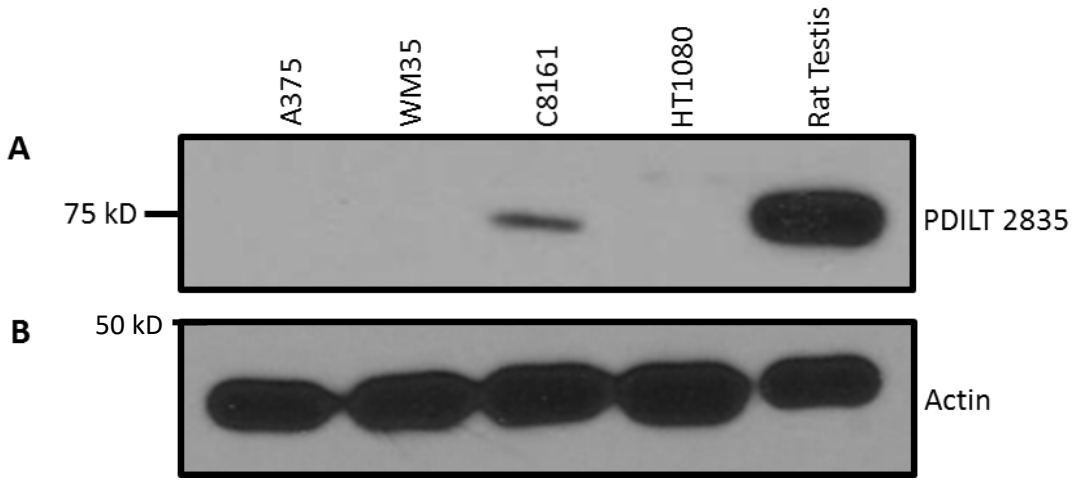

Figure 14: Western Blot of Melanoma Cell Lysates using a PDILT Antibody. Melanoma cells were lysed with MNT lysis buffer, run on an SDS-PAGE gel, transferred to PVDF and the membrane blotted with a PDILT antibody (2835) (Panel A) and an actin antibody (Panel B). An HT1080 lysate acted as a negative control and a rat testis lysate acted as a positive control for PDILT. The PDILT antibody (2835) revealed a positive band around the 75 kD mark, which migrated at the same position as the positive control, suggesting C8161 cells express PDILT. The actin blot (Panel B) confirmed equal loading of the proteins in the lysates.

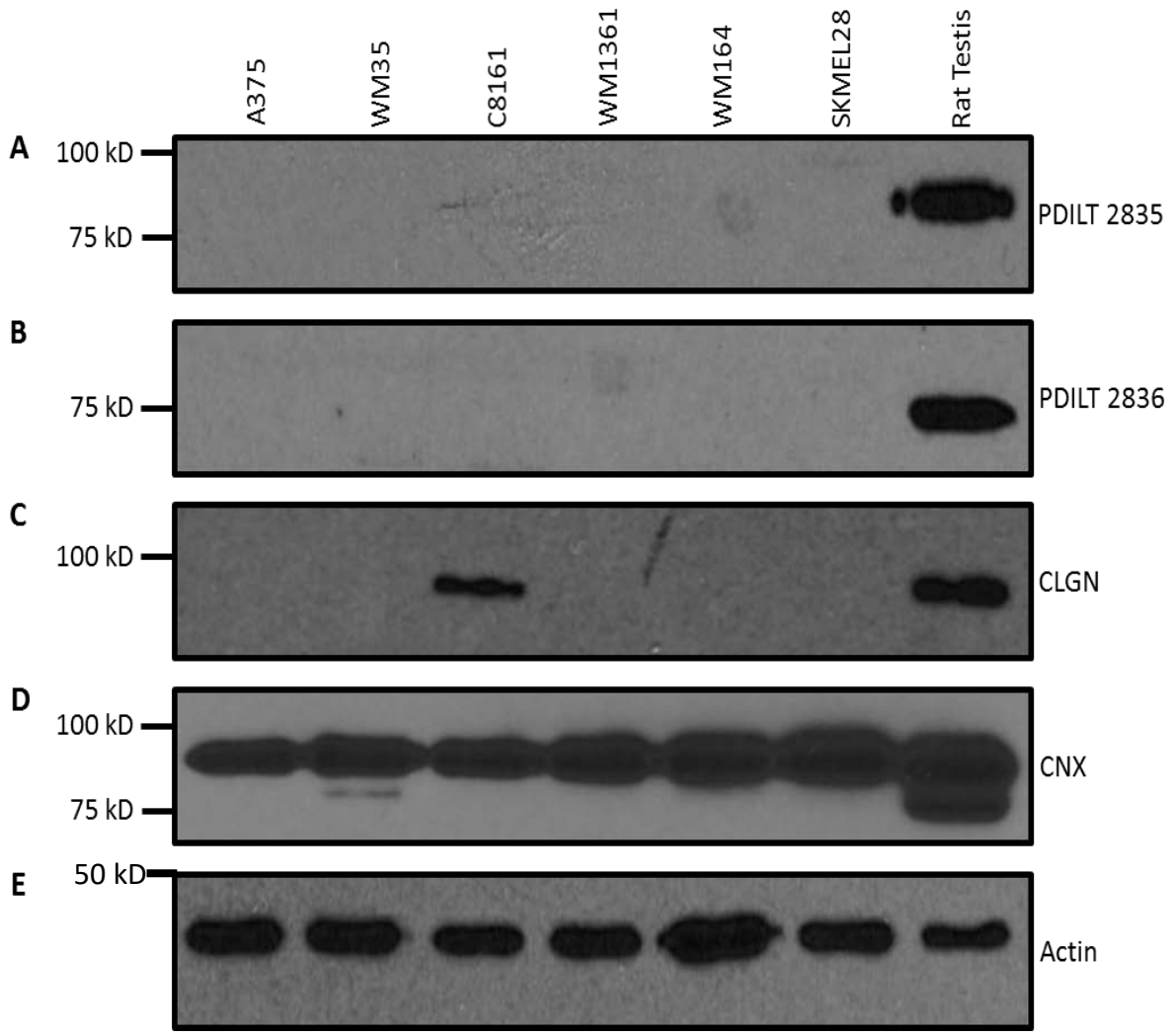

Figure 15: Western Blot of Melanoma Cell Lysates testing for a Variety of ER Proteins. Melanoma cells were lysed with MNT lysis buffer, run on an SDS-PAGE gel, transferred to PVDF and the membrane blotted with two PDILT antibodies (2835 and 2836) (**A** and **B**), a CLGN antibody (**C**), a CNX antibody (**D**) and an actin antibody (**E**). A rat testis lysate acted as a positive control. When blotting with the PDILT 2835 antibody and the PDILT 2836 antibody, none of the melanoma cell lysates returned a positive result, suggesting that none of the melanoma cells expressed PDILT. When blotting back with the CLGN antibody, a single band formed in the C8161 cell lysate lane around 80 kD (Lane 3), which corresponded to the band in the positive control. This suggests that C8161 expresses CLGN. All of the lysates expressed CNX when blotted with the CNX antibody. However, both the WM35 cell lysate and the rat testis cell lysate had a CNX doublet. The actin blot back showed a reasonable level of equal loading between all lanes.

4.2 Confirming Calmegin Expression in the C8161 Melanoma Cell Line

Following on from the observation that the C8161 cell line did express the testis specific ER protein calmegin, further testing was conducted to confirm the expression of calmegin and to explore the characteristics of its expression.

To confirm the expression of calmegin in the C8161 cell line, a C8161 cell lysate was compared against a WM164 cell lysate (a negative control due to its observed lack of calmegin expression) and against a rat testis lysate, which acts as a positive control. The lysates were run on an SDS-PAGE gel and blotted with two CLGN antibodies, one was a gift from M. Okabe, Osaka, and the other was commercially available (abcam, ab172477) from abcam. The CLGN antibody (abcam, ab172477) was used to confirm the initial identification of calmegin. As shown in Figure 16, both CLGN antibodies detected a band at ~100 kD in the C8161 lysate, in agreement with the positive control. However, the Okabe laboratory CLGN antibody gave a signal that had a slight reduction in molecular weight when compared to the positive control. The actin blot shows that there was mostly equivalent loading of sample between the lanes.

To further test CLGN and PDILT expression and to examine cellular localisation of CLGN, an immunofluorescence experiment was carried out (Figure 17). Both C8161 and WM164 cells were grown on cover slips, fixed, permeabilized and then incubated with either a PDILT 2835, CLGN or CNX antibody, followed by the donkey anti-rabbit secondary Alexa 594. The cells were also co-stained with DAPI to allow for nuclear identification. The results were consistent with what was observed in Figure 15. When both cell lines were incubated with the PDILT 2835 antibody, neither of the cell lines showed any cellular staining for PDILT. However, when both cell lines were incubated with the CLGN antibody, only the C8161 cell line demonstrated staining. This adds further evidence that C8161 expresses CLGN and also that it localises to the ER, as the staining in the cell was perinuclear in nature. The WM164 cell line had no CLGN staining and this observation was consistent with the previous western blotting result seen in Figure 15. When the cells were incubated with the CNX antibody, both cell lines had perinuclear staining, as expected given the normal ER localisation of CNX.

From this series of experiments it was clear that the C8161 cell line expressed calmegin and it localised to the ER, given the results from the western blotting and immunofluorescence experiments. The expression of PDILT in the melanoma cell lines is less clear. Given the difference in passage number from the positive result (Figure 14) and negative result (Figure 15), it is possible that PDILT is only expressed in the C8161 cell line when at a low passage. This should be examined in the future with C8161 lysates originating from different passage numbers analysed for PDILT expression.

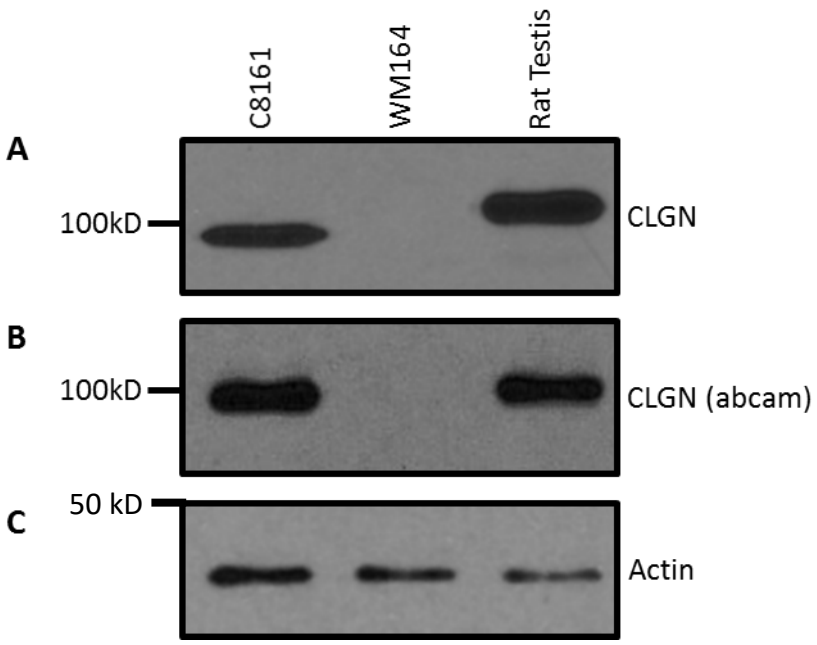

Figure 16: Western Blot Confirming Calmegin Expression in C8161 Cells. The C8161 lysate and the WM164 cell lysate produced for Figure 15 were rerun on an SDS-PAGE gel and western blotted with two independent CLGN antibodies (**A** and **B**). A rat testis lysate was used as a positive control. In (**A**), the C8161 cell lysate was positive for CLGN but the protein appeared to run at a lower molecular weight in comparison to the positive testis control. In (**B**) C8161 was also positive for CLGN, but the molecular weight more closely matched the positive control. The lack of reactivity in CNX-positive WM164 cells demonstrates that the CLGN antibody does not cross-react with CNX. The actin antibody (**C**) demonstrated equivalent loading between lanes.

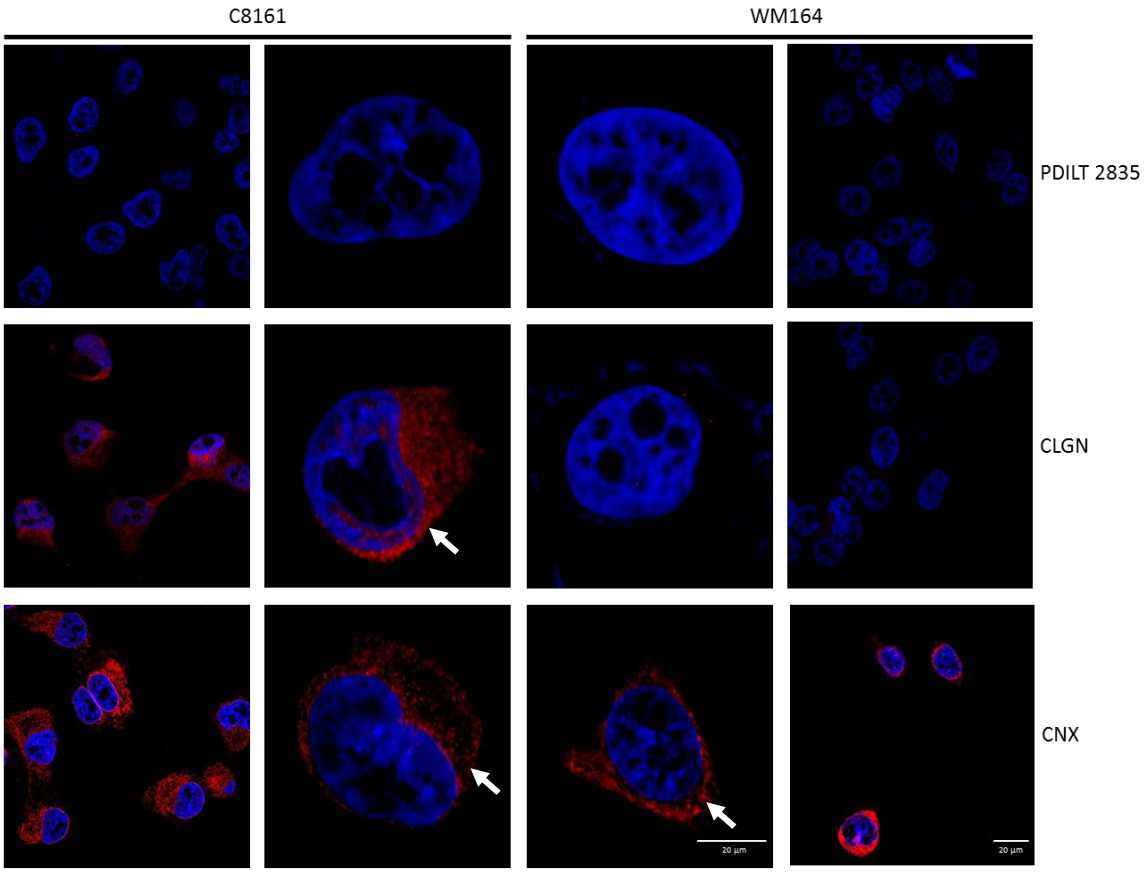

Figure 17: Immunofluorescence of C8161 and WM164 Cells. C8161 and WM164 cells were grown on 18 mm coverslips, fixed, permeabilized and then incubated with a PDILT antibody (2836) (**A B G H**), a CLGN antibody (**C D I J**) and a CNX antibody (**E F K L**). These cells were then imaged at ×63 magnification and at ×100 magnification with a Zeiss Apotome. Neither the C8161 nor the WM164 cells showed any staining for PDILT. Only the C8161 cells showed perinuclear staining for CLGN, consistent with ER localisation. The WM164 cells showed no CLGN staining, consistent with previous experiments. Both the C8161 and WM164 had perinuclear staining for CNX, as expected for a ubiquitously expressed ER protein. White arrows indicate positive expression. The scale for the 63x and 100x magnification images is 20µm.

4.3. Characterising Calmegin Expression in Mutant BRAF Melanoma Cell lines

Interestingly, C8161 was the only cell line analysed with a wild type form of BRAF (Information provided by Prof P. Lovat). Cell lines A375, WM164 and SKMEL have the melanoma mutation of V600E BRAF and WM35 cell line has a V599I mutation in BRAF. This genetic difference could explain why only the C8161 cell line expresses CLGN. This difference could allow for the potential targeting of CLGN for wild-type BRAF melanoma drug treatment, given that wt BRAF melanomas are resistant to current drug therapies. To examine whether other wt BRAF cell lines also demonstrate CLGN expression another wild type BRAF cell line, CHL1, was obtained for further testing. The cells were grown in 6 cm dishes alongside the C1816 and WM164 cells and lysed with MNT lysis buffer. The lysates were run on an SDS-PAGE gel alongside two melanocyte lysates with different pigmentation levels, light and dark. The melanocytes were analysed to test if normal melanocyte cells express CLGN. A rat testis lysate was used as a positive control. The proteins from the gel were transferred to a PVDF membrane which was probed with a CLGN antibody and an actin antibody (Figure 18). Both the C8161 and the CHL1 lanes had positive bands around 80 kD, corresponding to the positive band in the rat testis positive control lane. This lends more evidence to the hypothesis that the expression of CLGN correlates with melanoma cells that maintain a wild type form of BRAF. The WM164 lysate was negative for CLGN expression, which concurred with the previous results. Both the light and dark pigmented melanocyte lysates were negative for CLGN expression. This suggests that the expression of CLGN observed in both the C8161 and CHL1 cell line occurs post cancer initiation. The actin blot demonstrated a reasonable level of protein loading between lysates.

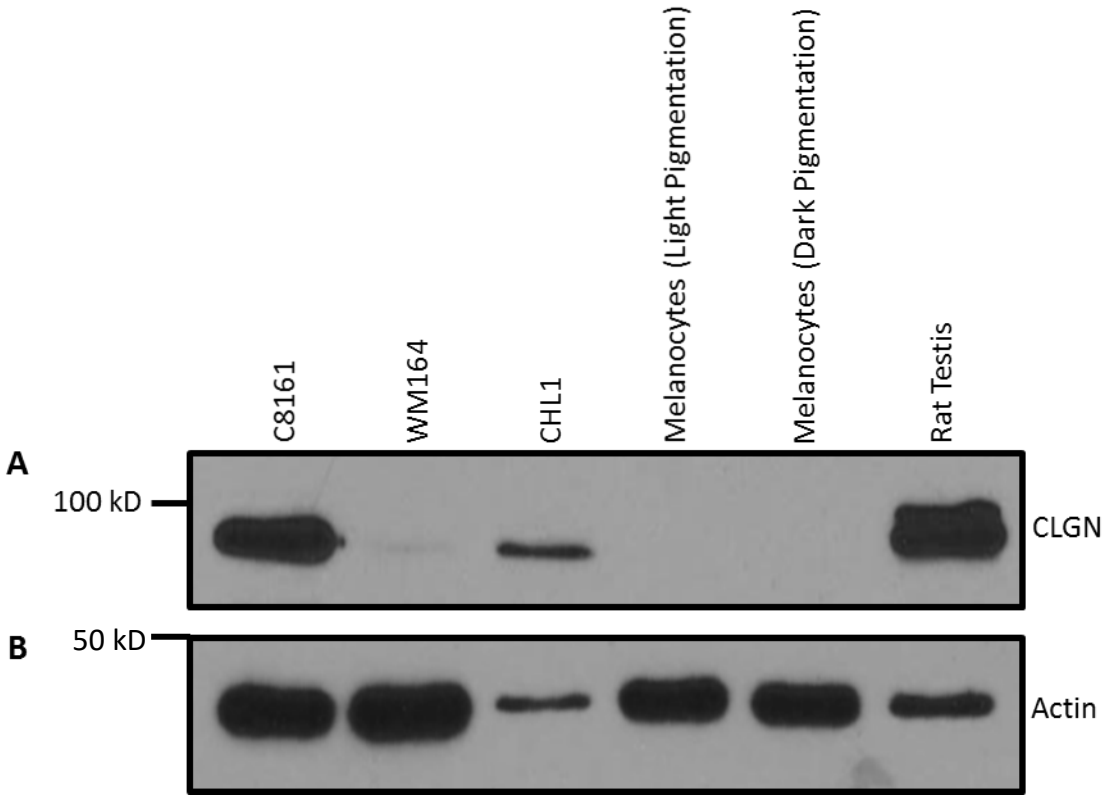

Figure 18: Examining CLGN Expression in WT BRAF Melanoma Cell Lysates and Melanocyte Lysates. Melanoma cells and melanocyte cell pellets were lysed with MNT lysis buffer and run on a SDS-PAGE gel. The proteins were transferred to a PVDF membrane and immunoblotted with (**A**) a CLGN antibody (abcam, ab172477) and (**B**) an actin antibody. A rat testis lysate acted as a positive control. Both of the C8161 and CHL1 lysates were positive for CLGN expression whereas the melanocytes did not express CLGN. The actin blot shows that the CHL1 cell expression of CLGN is likely to be underestimated given the unequal loading between CHL1 and the other samples.

Previous research on the relationship between ER stress and cancer has shown that the expression of certain ER proteins, such as GRP 78/BiP and GRP94 in colon cancer, acts to reduce ER stress and thus avoid self-induced apoptosis of the cell. It has also been shown that general ER stress, such as environmental stress, acts to upregulate these proteins (Welch 1992). In order to explore this, C8161 cells and WM164 cells were grown in spheroid culture and incubated for 4, 6 or 8 days. This was done to induce a hypoxic core at the centre of the spheroid. The resultant spheroids were then lysed and run on an SDS-PAGE gel for western blotting or fixed in paraffin and then subject to immunofluorescence following antigen retrieval. The western blotting data is shown in Figure 19. Lysates were produced by lysing 10 spheroids per sample in MNT lysis buffer, harvested at each of the different time points. For the western blotting experiments, these lysates were compared against a monolayer lysate from each of the cell lines. A rat testis lysate was also used as a positive control. Each set of samples was blotted with a CLGN antibody (abcam, ab172477), a PDILT antibody (2835) and the actin antibody.

Figure 19A shows that only the C8161 cell line was positive for CLGN and that regardless of the time point of harvesting, there was a consistent equal expression of CLGN. This suggests that neither the increased environmental stress from hypoxic conditions nor the spheroid morphology of the cells impacted on the expression of CLGN. The WM164 spheroids showed no expression of CLGN at any time point, suggesting that neither spheroid morphology nor hypoxic conditions induced CLGN expression.

Figure 19B shows the expression data for PDILT using the PDILT 2835 antibody. Neither the C8161 nor the WM164 cell line, regardless of time point of spheroid harvesting, had any detectable expression of PDILT. This concurs with previous results and it also suggests that neither spheroid morphology nor hypoxic conditions induces PDILT expression in either cell line, at least at later passage numbers. Figure 19C shows the expression of actin and indicated that there was a reasonably equal level of protein loading between the lanes.

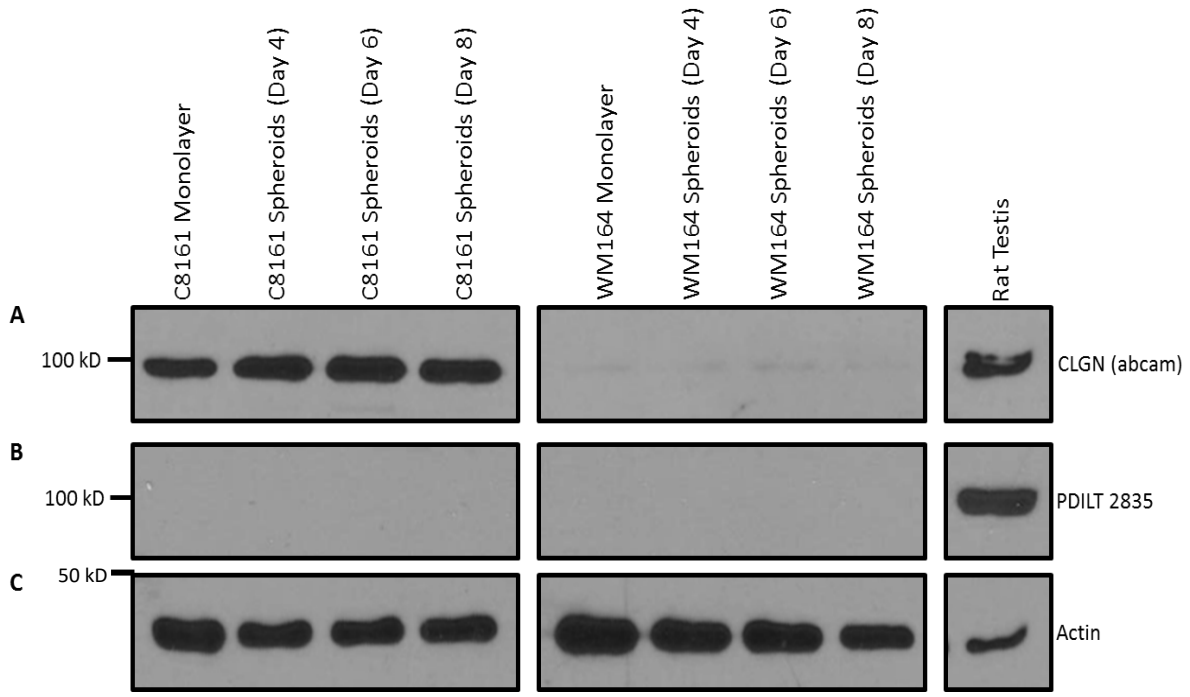

Figure 19: Western Blot of C8161 and WM164 Melanoma Spheroids. The C8161 and WM164 cell lines were used to produce spheroids which were harvested at days four, six and eight. Ten of these spheroids were isolated and lysed with an MNT lysis buffer and run on an SDS-PAGE gel. Lysates from monolayers of each of the cell lines were also ran to control for the spheroid morphology. A rat testis lysate acted as a positive control. The resultant western blot was probed with a CLGN antibody (abcam, ab172477) (**A**), a PDILT antibody (2835) (**B**) and an actin antibody (**C**). When blotting with the CLGN antibody, all the C8161 lysates showed expression of CLGN, having a band form around the 100 kD mark that matched the positive control. However, there was no difference in level of CLGN expression between any of the spheroids or the monolayer lysate. None of the WM164 lysates demonstrated CLGN expression, consistent with previous results. When blotting back with the PDILT antibody, none of the lysates showed PDILT expression. The data shows that neither spheroid morphology nor hypoxic conditions can induce PDILT or CLGN expression in either melanoma cell line. The actin blot shows equivalent levels of protein loading between samples

Spheroids were also harvested for immunofluorescence. Spheroids were imbedded into agar, and then imbedded into paraffin. The resultant paraffin blocks were sectioned and then subject to antigen retrieval with 74.4 mM sodium citrate. Post antigen retrieval, each of the sections were incubated with either no primary antibody, a PDILT antibody or a CLGN antibody. They were also incubated with the donkey anti-Rabbit secondary Alexa 568 and DAPI to stain cell nuclei. The results are shown in Figure 20. The C8161 spheroids, regardless of the time point of harvesting appeared to express a similar level of calmegin, as judged by staining around the periphery of the spheroid. One possibility is that the expression of CLGN only occurred at the external of the cell due to loss of CLGN expression at the hypoxic core of the spheroid. However, there was also some peripheral staining of PDILT. Given the lack of PDILT staining from the western blotting data for both cell line spheroids and the lack of a positive control (i.e. a spheroid of HT0180 cells transfected PDILT), the peripheral staining obtained in these experiments is unlikely to be genuine.

The WM164 spheroids (Figure 21) showed no detectable CLGN expression at any time point, as there was no staining in any part of the spheroid. Similar to the C8161 spheroids, the results seem to suggest that PDILT is expressed in the WM164 spheroids as there was similar staining at the periphery of the spheroid. For the WM164 spheroids, the spheroids incubated with no primary antibody produced poor quality images. This made ascertaining the expression of different proteins difficult. Further experiments with additional controls would be required to definitively confirm whether or not PDILT is expressed in spheroids derived from different melanoma cell types.

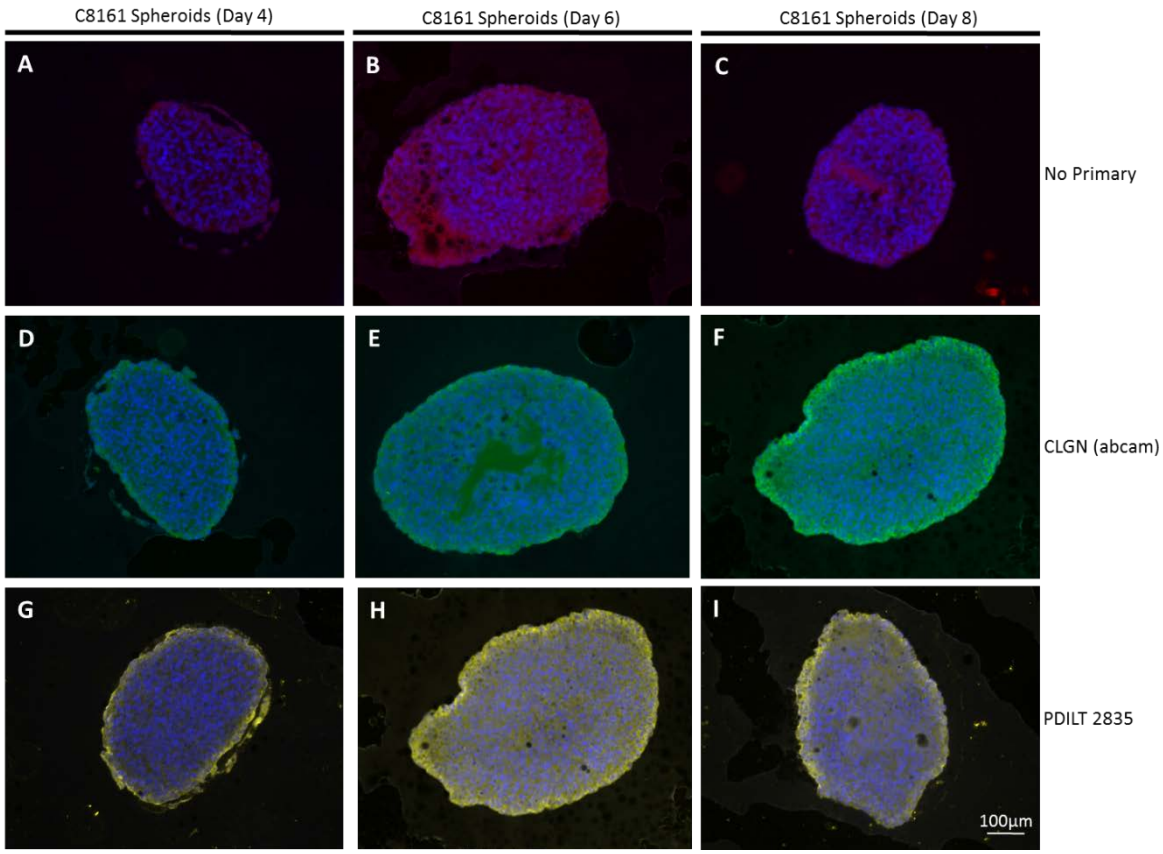

Figure 20: Immunofluorescence of C8161 Melanoma Spheroids. Embedded spheroids of the C8161 cells were sectioned, subject to antigen retrieval and incubated with either no primary (**A**-**C**), a CLGN antibody (abcam, ab172477) (**D**-**F**) or a PDILT 2835 antibody (**G**-**I**). The sections were then imaged at ×20 magnification with a Zeiss 880 microscope. The C8161 spheroids incubated with the PDILT antibody showed some peripheral staining, suggesting that the spheroid expressed PDILT at the periphery. When incubated with CLGN, the same peripheral staining was observed. The scale for the 20x magnification images is 100µm.

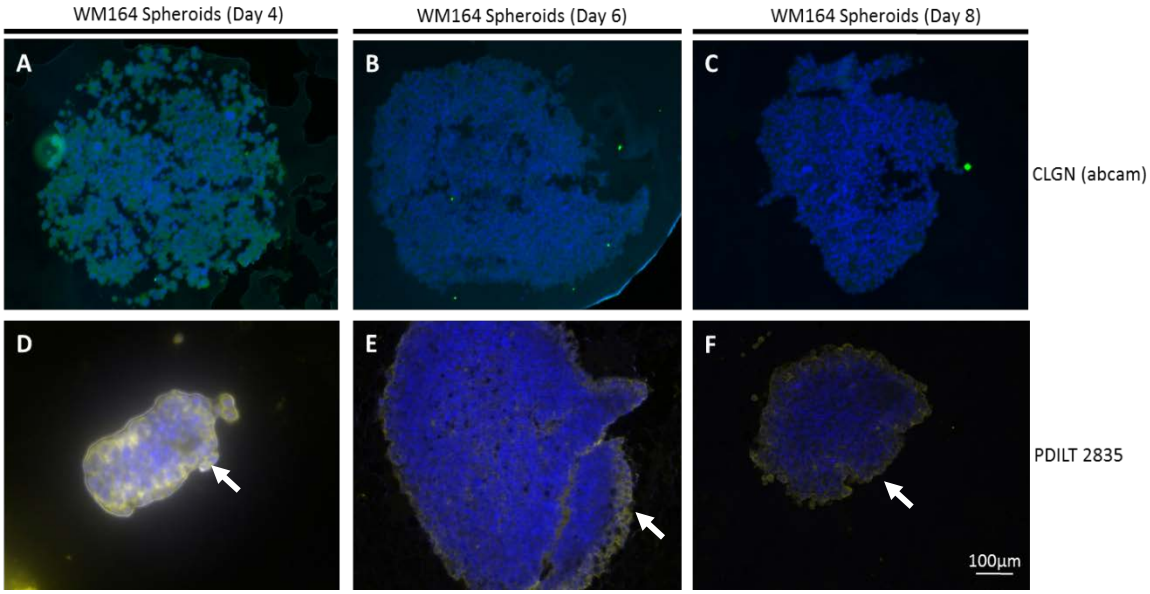

Figure 21: Immunofluorescence of WM164 Melanoma Spheroids. Embedded spheroids of the WM164 cells were sectioned, subject to antigen retrieval and incubated with a CLGN antibody (abcam, ab172477) (**A**-**C**) or a PDILT 2835 antibody (**D**-**E**). The sections were then imaged at ×20 magnification with a Zeiss 880 microscope. The WM164 spheroids showed no expression for CLGN. However, the WM164 spheroids showed similar peripheral staining for PDILT that was seen in the C8161 spheroids, suggesting that the spheroid expressed PDILT at the periphery. White arrows indicate positive expression. The scale for the 20x magnification images is 100µm.

4.4. CLGN and PDILT Expression in Human Melanoma Tumours

To examine if the expression of CLGN that was observed in wild type BRAF melanoma cell lines also occurs in human melanoma tumours, several human tumours of different BRAF mutational states were examined by immunohistochemistry. The mutational status of these tumours is listed in Table 3. These tumours were already imbedded in paraffin and were thus sectioned and mounted on slides, subject to antigen retrieval with sodium citrate and incubated with the two PDILT antibodies (PDILT 2835 and 2836) and the commercial CLGN antibody. The tumours were also costained with DAPI to allow for nuclear identification (Figure 22). Each of the tumours, regardless of the antibody used, had a pattern of dispersed staining that was not cell specific. This was likely caused by either using too high a concentration of primary or secondary antibody, or arose from incomplete blocking. Due to the lack of specificity in the antibody signal, it was not possible to determine whether CLGN or PDILT was expressed in any of these tumours. This series of experiments should be repeated following an optimisation of the antibodies and antigen retrieval method.

However, taken together, the data presented in this results chapter suggests that CLGN is likely to be expression in some human melanoma and it remains possible that PDILT is also expressed in this malignancy.

.

Table 3: Human Melanoma Tumours

List of all tumours used in experiments. Each tumour has information regarding the sex of the patient, the age of the patient when the tumour was extracted, the stage of the tumour and its mutational states regarding BRAF and NRAS.

Tumour Name	**Tumour Type**	**Sex of Patient**	**Age of Patient**	**ACC Tumour Stage at Diagnosis**	**BRAF**	**NRAS**
M018	Melanoma	F	42	IIA	wt	wt
M040	Melanoma	F	58	IIA	wt	wt
M044	Melanoma	F	48	IB	V600E	wt
M045	Melanoma	M	26	IIC	V600E	wt
M046	Melanoma	M	35	II	V600E	wt

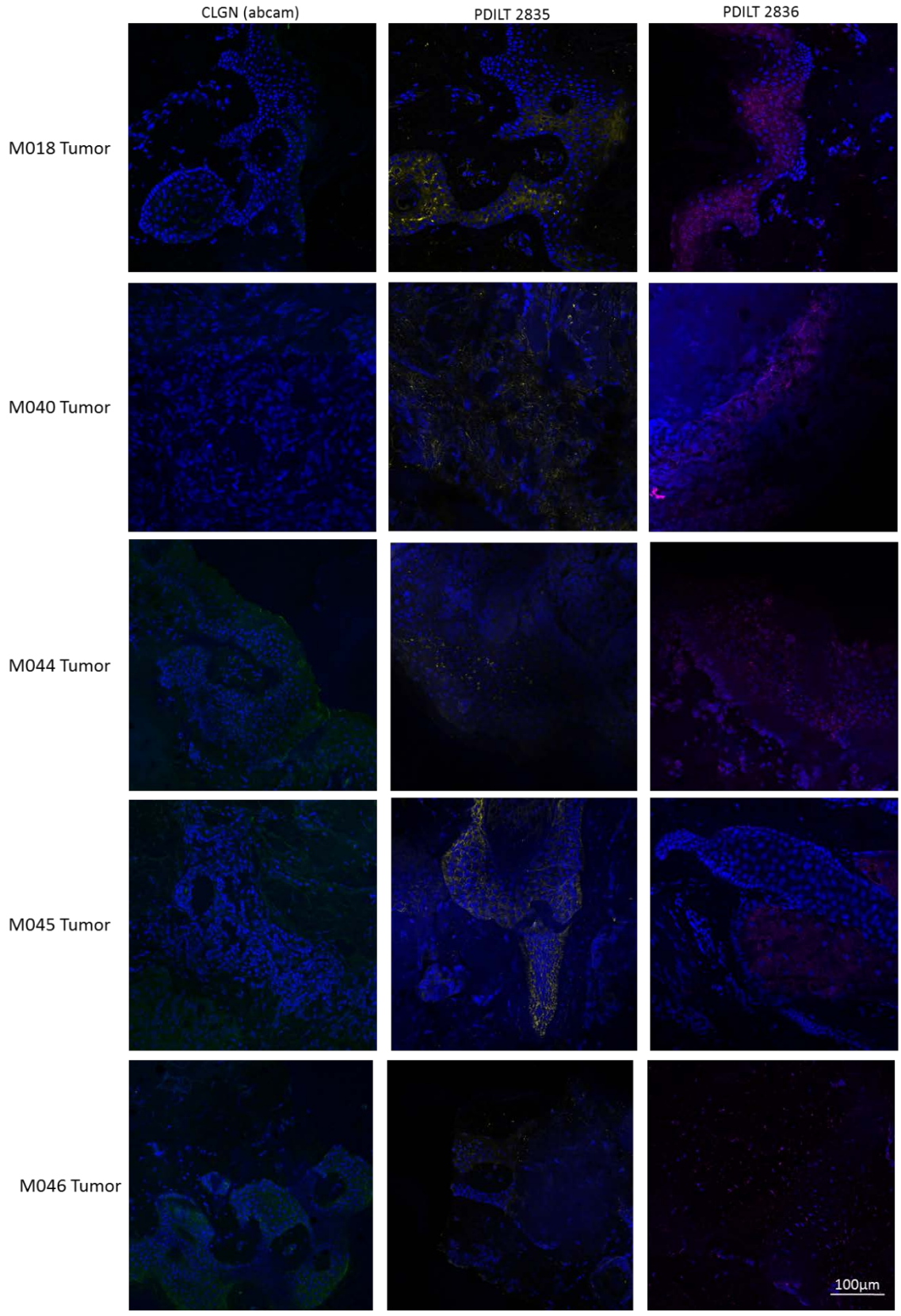

Figure 22: Immunofluorescence of Human Melanoma Tumours. The paraffin imbedded tumours were sectioned, subject to antigen retrieval and incubated with both the 2835 and 2836 antibody and the CLGN antibody. The scale for the 20x magnification images is 100µm.

5. Discussion:

5.1 Expression of PDILT in HT1080 cells

This thesis began with examining the expression of transfected constructs in HT1080 cells. The ability of HT1080 cells to express PDILT was confirmed firstly by western blotting (Chapter 3.1 – Figure 7) and by immunofluorescence (Chapter 3.1 – Figure 8). However, it was noted that the transfection efficiency in the initial immunofluorescence experiments was relatively poor, being only around 5 %. Transfection efficiency is influenced by a number of different factors, with one of the most prominent factors being the ratio of nucleic acid to transfection reagent (Kim and Eberwine 2010). To investigate if this impacted on the success of the transfection, different volumes of vector and transfection reagent were used (chapter 3.2 – Figure 9). It was found that using 2.50 ug of cDNA and a lipofectamine volume of either 3.75 µl or 7.5 µl gave the highest transfection efficiency. These experiments demonstrated that HT1080 cells are suitable cells for the expression of PDILT and transfection of PDILT constructs. However, the relatively poor transfection efficiency suggests that generating stable transfected cell lines for the study of PDILT mutants should be addressed in the future. An alternative solution is to develop an immortalised cell line from testis that can stably express PDILT, as this would eliminate the issues surrounding transfection, such as the need to validate successful transfection and the variable transfection efficiency. However, attempts to establish stable post-meiotic germ cells in culture have not been possible by any laboratory up to now (Staub 2001).

5.2 Mutations to Key Structural Elements of PDILT Impact on its Ability to Interact with Client Proteins

In this thesis, an analysis was carried out on proteins lacking the C-terminal domain and proteins lacking two key cysteines present in PDILTs structure. How these elements contribute to the ability of PDILT to bind to client proteins in the ER was investigated. van Lith et al. 2004 described several differences between PDILT and the classical PDI protein structure. Two of these identified differences between PDILT and PDI are the two cysteines present in PDILT, at position 135 and 420, one of which is away from the oxido-reductase active site. These cysteines were targeted for study by substitution (to alanine) because they are solvent exposed and previously suggested to play a role in binding to client proteins (van Lith et al. 2007). The other major difference between PDILT and the PDI is the large C-terminal extension, which increases the size of the protein to 67 kDa. Thus deletions at two

different positions (498 and 520) were studied. The “tail” mutants were also combined with the cysteine mutants. The cDNAs used in this study, including constructs kindly provided by the Nagata laboratory, are summarised in chapter 3.1 – Figure 6. It has previously been shown by van Lith and Benham that myc-tagged PDILTC135A and Myc-tagged PDILTC420A displayed altered disulphide-dependent binding to putative client and co-chaperone proteins (van Lith et al. 2007). In this thesis, the behaviour of FLAG tagged PDILTC135A and Flag tagged PDILTC420A was investigated to address whether the nature of the tag influenced the interactions, and to validate alternative PDILT cDNA reagents. The FLAG tagged mutant proteins were analysed by western blotting, to observe how each of the individual mutations effected PDILTs ability to form disulphide dependent interactions with client proteins (Chapter 3.2 – Figure 10 and 11).

The WT FLAG tagged PDILT protein formed high molecular weight complexes around 250 kDa under non-reducing SDS-PAGE and showed the presence of a high number of PDILT/client complexes, as expected from the literature (van Lith et al. 2007). The single cysteine substituted mutants, C135A and C420A, both saw a reduction in size of the high molecular weight bands, consistent with results obtained with the equivalent myc-tagged constructs. Whilst there was a loss of some client interactions, there was not a total abolishment of all interactions. This concurs with the results presented in van Lith et al. 2007. However when both cysteines are substituted out, in the C135A/C420A mutants, there was a total abolishment of all disulphide dependent client interactions. This demonstrated that all detectable client interactions through disulphide bonds are mediated by the solvent-exposed cysteines present at position 135 and 420. The two tail deleted PDILT mutants, PDILT DEL 498-580 and PDILT DEL 520-580, caused the formation of more bands over a large kDa range, suggesting that there was an increase in the number or extent of client interactions. From this finding, it is plausible to suggest that the tail of PDILT may regulate the interaction between PDILT and client proteins, as there was a large increase in the number of interactions once it was removed. However, it is also possible that the tail-deleted PDILT constructs misfold to some extent and are targeted to alternative disulphide-dependent interactions involved in ER protein folding and degradation.

When the cysteine mutations were combined with the tail deletions DEL 498-580+C135A/C420A and DEL 520-580+C135A/C420A, there was a complete absence of a high molecular weight band, suggesting that all disulphide dependent client interactions were abolished. This is to be expected and demonstrates that the tail does not mediate disulphide dependent interactions away from the two solvent exposed cysteines. The monomer form of

PDILT was seen in the majority of the mutants, but monomer bands were absent for the PDILT WT and PDILT DEL498-580 mutants. This lack of detection could be explained by possible degradation of the translated mutants. This is possible because both of these mutants contain the FLAG tag and the PDILT DEL498-580 mutant had part of its C-terminal deleted. These structural alterations could impact on the folding of these mutants to such an extent that they become targeted for degradation by the ER surveillance machinery. However, the lack of bands could be explained by experimental issues, such as an air bubble forming (during transfer) over the same area as the expected weight area of PDILT monomers of these mutants.

The cellular localisation of PDILT was also explored with a series of immunofluorescence experiments in HT1080 cells (chapter 3.2 – Figure 12 and 13). Regardless of the PDILT construct, there was a strong level of perinuclear staining for successfully transfected cells. From this result, it can be concluded that the FLAG tag does not interfere with ER localisation of PDILT, tail and that C135A, C420A and the tail are not required for localising PDILT to the ER of the cell. However, co-staining with a range of ER protein markers, and the use of higher resolution microscopy, will be required to determine whether there are any differences in localisation to putative ER domains. Interestingly, there was also some punctate staining throughout some of the transfected cells, with the clearest example of this seen in the cells expressing PDILT DEL 520-580+C135A/C420A shown in Chapter 3.2 - Figure 13. This observation could explain some of the loss of the monomer forms seen in the accompanying western blots, if the mutated proteins were identified as misfolded proteins and trafficked for degradation along the autophagic/lysosomal pathway. Further co-localisation experiments with lysosomal/ERAD/autophagic markers would be required to investigate this possibility.

5.3 Calmegin is Expressed in WT BRAF Melanoma Cell Lines

This thesis also investigated the possibility that PDILT was expressed in melanoma cells, following on from the observation that a selection of tumours in the Human Protein Atlas, sourced from both males and females between the ages of 50-80, stained positive with an antibody raised against PDILT. Six melanoma cell lines were donated by Prof Lovat and these cell lines were grown to confluency, lysed with an MNT lysis buffer and analysed by SDS-PAGE and Western blotting.

Initially, only three of the cell lines were tested for PDILT expression using a PDILT antibody (2835). Of the three cell lines tested, only the C8161 cell lysate demonstrated expression of PDILT (Chapter 4.1 – Figure 14). In order to confirm this expression, all six melanoma cell lines were analysed. The resultant gels were blotted using two distinct PDILT antibodies and a variety of other ER protein antibodies. Immunoblotting with the two PDILT antibodies, 2835 and 2836, revealed that none of the cells expressed PDILT (Chapter 4.1 - Figure 15). The difference could be down to the difference in passage number of the C8161 cells. It was noted that in Chapter 4.1 – Figure 14, C8161 were lysed whilst at a low passage number (passage 10) and in Chapter 4.1 – Figure 15, were lysed whilst at a high passage (passage 27). This remains to be confirmed by direct comparison between C8161 cells at different passage numbers but this could suggest that PDILT is induced in melanoma tissue *in situ*, but fades *in vitro* over time. However, whilst PDILT expression in these melanoma cell lines remains inconclusive, analysis with a CLGN antibody revealed that CLGN was definitely expressed in the C8161 cell line. CLGN is also an ER resident protein that was identified as a key mediator of spermatogenesis. Rats immunized to testis cells had the resultant antibodies purified and used to identify different proteins involved in the male reproductive process (Watanabe et al. 1993). This led to the characterisation of CLGN and further work in mice identified that CLGN -/- sperm both failed to bind to the membrane of the zona pellucida or migrate into the oviduct (Ikawa et al. 2001). This protein also has been linked to certain cancers, for example CLGN has been suggested to be expressed in breast cancer following bone metastasis (Smid et al. 2006). Thus the identification of this protein in C8161 cells is novel but logical. When probing the melanoma cell lysates with the CNX antibody all cell lines tested showed expression of CNX, which is to be expected given the universal expression of the protein across all cell types. So whilst PDILT does not appear to be expressed in the majority of melanoma cell lines, it does appear that CLGN is expressed in the C8161 cell line.

The observation that the C8161 cell line expresses CLGN was confirmed by immunoblotting with a commercially available antibody (Chapter 4.1 – Figure 16). To further explore the expression of CLGN and other ER proteins, a series of immunofluorescence experiments were carried out on C8161 cells (Chapter 4.2 – Figure 17). C8161 did show staining for CLGN in a perinuclear location. This suggests that CLGN is localised to the ER of the C8161 cells, but a more extensive colocalisation study with a range of known ER proteins would help to extend these observations. The lack of PDILT staining in the C8161 cell line suggests that either PDILT is not expressed in this melanoma, or there is passage dependent downregulation of PDILT expression when cells are cultured.

Following on from the observation that the C8161 cell line expresses CLGN, it was then investigated to see if CLGN expression was specific to the C8161 cell line or if this expression was linked to the genetic profile of the C8161 cell line. One of the most frequent mutations in melanoma is a V600E mutation occurring in BRAF, a serine/threonine kinase protein involved in the MAP signalling cascade, with a mutation occurring in this protein in 50 % of melanoma (Ascierto et al. 2012). This signalling cascade is shown in Figure 23. The C8161 cell line was the only cell line to have a wild type form of BRAF and NRAS. In order to test if other melanoma cell lines with this genetic profile also express CLGN, CHL1 cells were also tested for CLGN expression and found to be CLGN positive (Chapter 4.2 – Figure 18). This suggests that melanoma cell lines that maintain a WT BRAF and a WT NRAS during their cancer progression express CLGN. Two melanocyte cell types were assessed to ascertain whether CLGN expression is gained or lost following cancerous transformation. Neither the lightly pigmented nor the heavily pigmented melanocyte lysates showed a positive result for CLGN expression, demonstrating that CLGN expression occurs post melanocyte transformation. This is potentially significant as it has been noted that unlike melanomas carrying mutations in BRAF, which are treatable with drugs such as vemurafenib (Sosman et al. 2012) or dabrafenib (Hauschild et al. 2012), WT BRAF melanomas are refractory to current drug treatments. Thus, evidence that WT BRAF melanoma cell lines express a novel ER resident chaperone protein, post transformation, lays the ground work for exploring CLGN (or its clients) as a possible therapeutic target. However, before this can be done, a more extensive analysis of the contribution of this protein to maintaining or contributing to cancer cell fitness has to be conducted. The key factors to assess are whether CLGN contributes to the proliferation, migration, cell survival or metastasis of cancer cells. Given that CLGN is an ER protein involved in protein folding, it is likely that its upregulation could enhance the secretion of other proteins (such as growth factors or adhesion molecules) involved in these processes. Thus, it is possible that manipulating the expression or activity of CLGN could result in the attenuation of one or more these cancer cell processes.

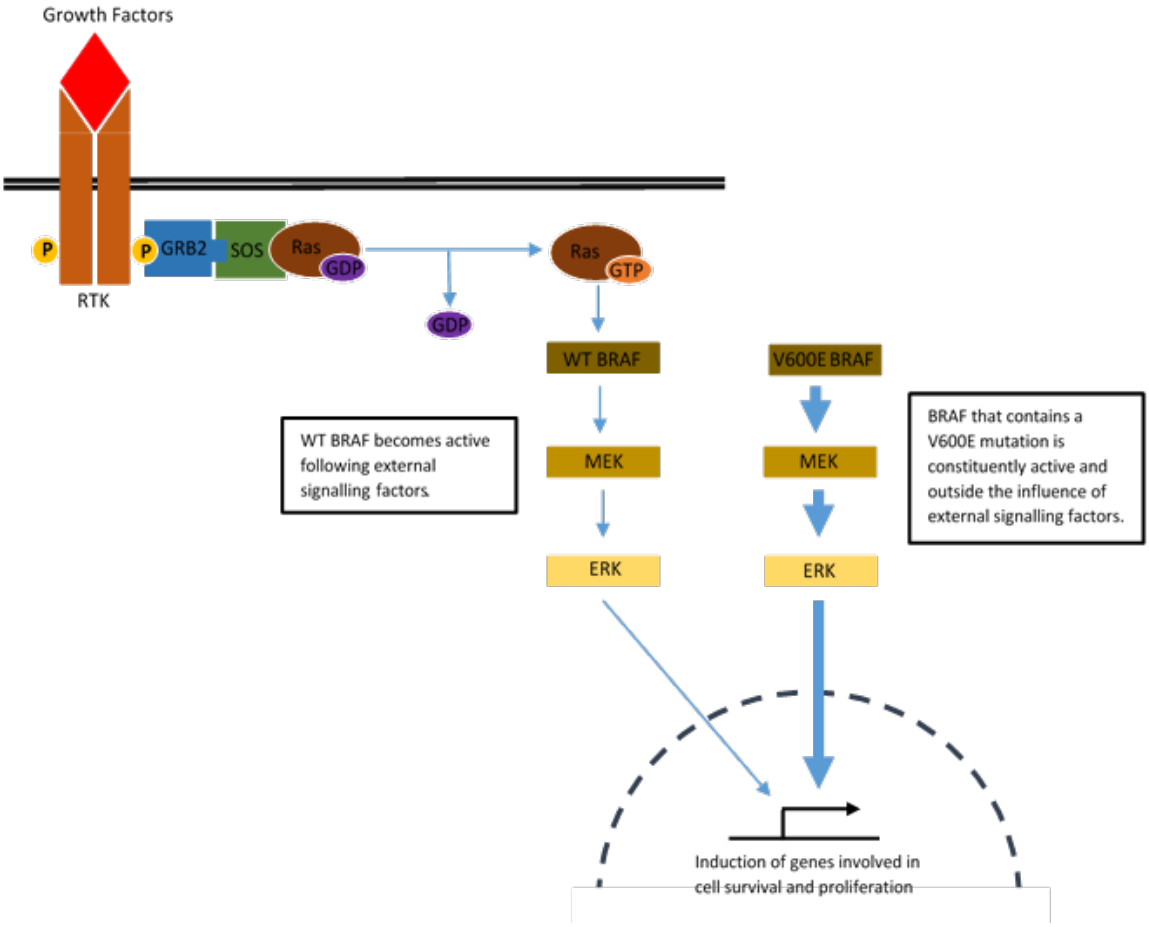

Figure 23. The MAP signalling cascade with WT BRAF and V600E BRAF. Under normal signalling conditions, growth factors such as EGF bind to the EGF receptor, which causes phosphorylation on its tyrosine residues. That allows GRB2 and SOS to bind in a complex to the EGFR. SOS becomes activated which allows Ras to bind to the complex. This causes the GDP bound to Ras to dissociate, allowing GTP to bind to it, which then activates Ras. Activated Ras can activate MEK, which then activates ERK. This signal transduction cascade causes the induction of genes involved in cell survival and proliferation. An issue arises when BRAF has a V600E mutation, which causes the protein to be constitutively active, leading to constant activation of MEK and ERK and thus constitutive pro-survival and proliferation signalling.

5.4 Impact of Spheroid Morphology and Hypoxia on CLGN Expression

Having established the expression of CLGN in WT BRAF melanoma cell lines, the impact of a variety of factors on the expression of CLGN and other proteins was also explored. Two factors were analysed, namely 3D cell culture and hypoxia. Cells were grown as spheroids, as this 3D cellular arrangement encourages the development of a necrotic core due to the lack of an oxygen supply. C8161 spheroids were either analysed by western blotting (Chapter 4.3 – Figure 19) or imbedded into paraffin and subject to immunofluorescence (Chapter 4.3 – Figure 20 and 21).

Initial immunofluorescence of the spheroids revealed CGLN expression within the C8161 spheroids (Chapter 4.3 – Figure 20). In the C8161 spheroids there appeared to be some staining at the periphery of the outer cells, which was absent in the WM164 spheroids (Chapter 4.3 – Figure 21). It is possible that a combination of pro-survival signals secreted by the cell and pro-apoptotic signals from the necrotic core promotes CLGN expression. Unexpectedly, both the C8161 and WM164 spheroids appeared to show PDILT staining at the exterior of spheroid cells. This is most likely due to edge effects or secondary antibody staining and could be resolved using alternative PDILT antibody staining strategies.

Spheroids did not, at any time point, show any protein expression of PDILT. Thus, neither 3D arrangement of cells or hypoxic pressure from the necrotic core was able to induce the expression of PDILT. When the same spheroid lysates were blotted with the CLGN antibody, the C8161 spheroids showed consistent CLGN staining across all time points. This shows that neither 3D structure nor increasing hypoxic pressure alters the level of expression of CLGN. The CLGN negative WM164 cell line showed no expression of CLGN at any point when grown as spheroids. This demonstrates that neither 3D structure nor hypoxic pressure from the necrotic core was able to induce CLGN expression and was not able to alter the level of expression of the protein. This could be because the cell already expresses CLGN at the highest level. However, the level of hypoxia at the centre of each spheroid was not verified in these experiments. To further explore the effects of hypoxia, the spheroids could be stained for known markers of hypoxia, such as HIF1alpha. Alternatively, spheroids could be incubated in a hypoxic chamber for a predetermined amount of time and then analysed. Little is known about how the transcription of CLGN (and PDILT) is regulated in the testis. Thus it would also be informative to conduct promoter binding studies and perform chromatin immunoprecipitation assays (ChiP) to establish how these genes are expressed and repressed.

5.5 Calmegin Expression in Human Melanoma Tumours

Whilst the observation that CLGN is expressed in WT BRAF melanoma cell lines is of note, it is important to demonstrate whether this expression also occurs in human WT BRAF tumours, to realise any therapeutic potential of targeting this protein. Thus several human melanoma tumours were initially screened for CLGN and PDILT expression (Chapter 4.4 – Figure 22). Unfortunately, the preliminary results from this analysis were inconclusive because of incomplete antigen retrieval. Some staining was apparent in some of the sections, but appeared to be nonspecific as a result of edge effects. Thus, a full optimization of antigen retrieval should be carried out on a variety of human tumours to ensure that antigen retrieval is complete. Co-staining the tissue with a known melanoma marker, such as Melan A, would ensure that any positive staining for CLGN or PDILT could be co-localised with cancerous tissue.

5.6 Future Work

In this thesis, I have focused on two areas of investigation. The first was an analysis of how different structural elements of PDILT contribute to PDILTs client binding. This led to the theory that the C terminal tail of PDILT, which is extended in comparison to other proteins in the same family, regulates the interactions between PDILT and its client proteins. This suggested mechanism of action is consistent with the recently published crystal structures of PDILT (Yang et al. 2018) and should be further explored in future work.

One possible way of exploring this theory is to co-transfect cells with PDILT DEL 498-589 or PDILT DEL 520-580 mutants with constructs bearing their missing tail peptides. If increased expression/concentration of the tail fragment protein causes a decrease in the high molecular weight complexes forming (which could be tested by the western blotting method outlined in Chapter 3.2 – Figure 9), this would provide further evidence that the tail regulates client binding. Similar studies could be performed using an *in vitro* translation approach. Putative regulation could also be confirmed by carrying out quantitative mass spectrometry, and comparing the number of interactions with the PDILT tail deleted mutants to the number of protein interactions with the WT PDILTs. That would provide further quantitative proof that an increase in client interactions occurs and would add to the qualitative data provided by the western blots. It would also be interesting to assess whether there are any particular types of proteins (in terms of function or structural characteristics) that have increased binding compared to others when the tail is removed.

The second area of investigation conducted in this thesis examined whether melanoma cells express PDILT or CLGN. This thesis suggests that PDILT is probably not expressed in the tested melanoma cell lines, but has demonstrated that CLGN is expressed in melanoma cell lines that maintain a WT form of BRAF. This unique protein expression in this form of melanoma could be exploited therapeutically, as disrupting the function of CLGN within the cancer cell could lead to increased ER stress and ultimately apoptosis of the cell.

However, before the therapeutic potential of CLGN can be realised, a full understanding of how CLGN expression supports cancer cell growth must be understood. Future work should be focused on knocking out CLGN and analysing if this impacts on a variety of cancer activities, such as proliferation, migration and metastasis. It is possible that CLGN contributes to these cancerous activities indirectly, through ensuring the correct folding of other proteins involved in these processes. Cancers are able to upregulate proteins involved in proliferation, migration and cell survival but without ensuring these proteins can be correctly folded and trafficked, this would ultimately lead to increased ER stress and trigger UPR induced cell death. Thus, it is possible that CLGN could contribute to one or more of these cancerous activities, by ensuring particular client proteins are correctly folded. The impact of knocking down CLGN on proliferation could be analysed with a combination of MTT and MTS assays. The impact on migration could be analysed with the use of a collagen cell invasion assay or could be performed on skin equivalent models to understand the invasion in a more appropriate environment. Once these knockdown effects have been observed, targeting the protein with a variety of possible therapeutics can begin. However, another important area requiring research is the exact mechanism by which genes, such as CLGN, become derepressed during melanoma development. A combination of promoter binding studies and chromatin immunoprecipitation assays (ChiP) would begin to elucidate this process.

Work also needs to be performed to validate the expression of CLGN in human WT BRAF melanoma tumours, to ensure that results in the cell lines can be translated into patients.

5.7 Conclusion

In this thesis, the role of key structural elements of PDILT in facilitating client binding and the expression of PDILT and CLGN in melanoma cells has been explored.

This thesis has expanded on the work initially performed by van Lith and Benham 2007, exploring the role the cysteines and the C-terminal extension play in PDILTs ability to bind to

client proteins. It has added further evidence to the importance of the solvent-exposed cysteines present in PDILT in mediating disulphide based interactions with potential client proteins and also theorised on the role of the C-terminal extension. Our hypothesis is that the C-terminal extension regulates interactions between client proteins and PDILT. This additional knowledge of PDILT is important and this will hopefully lead to a more complete understanding of the molecular mechanisms of PDILT that underpin its role in male fertility, and may help us to understand how PDILT interacts with the sperm:egg binding protein ADAM3.

This thesis also explored the possibility that testis-specific ER chaperones are expressed in melanoma cells. The thesis has clearly shown that CLGN is expressed in the ER of melanoma cell lines that maintain a wild type form of BRAF and NRAS. This is potentially significant as current treatments of melanoma have shown to have limited long term efficacy (Flaherty et al. 2012). This is especially true in terms of treating melanomas that maintain a WT BRAF, as they currently lack any targeted treatment. Thus, further work proving CLGN expression in WT BRAF human melanoma tumours would open the possible therapeutic option of targeting this protein to induce UPR mediated apoptosis, which has already been demonstrated to be effective when targeting PDI (Lovat et al. 2008). However, the expression of CLGN in human melanoma needs to be validated in future. This previous work has demonstrated the effectiveness of targeting ER disulfide-isomerases as a melanoma treatment, but targeting other forms of ER processing such as the complex mechanism of glycosylation, have yet to be investigated as possible melanoma treatments. This approach could be built around further knowledge of the molecular mechanisms that allow melanoma cancer cells to survive and spread.

6. List of References:

Bastos-Aristizabal, Kozlov and Gehring (2014) Structure of the substrate-binding b' domain of the Protein Disulfide Isomerase-Like protein of the Testis, Scientific Reports, 4, 44464.

Benham (2012) The protein disulfide isomerase family: key players in health and disease. Antioxidants & Redox Signalling, 16(8), 781-789.

Benham, van Lith, Sitia and Braakman (2013) Ero1–PDI interactions, the response to redox flux and the implications for disulfide bond formation in the mammalian endoplasmic reticulum. Philosophical Transactions of the Royal Society B 368: 20110403.

Caballero and Chen (2011) Cancer/Testis Antigens: Potential Targets for Immunotherapy. Innate Immune Regulation and Cancer Immunotherapy, 347-369.

Cai, Wang and Tsou (1994) Chaperone-like Activity of Protein Disulfide Isomerase in the Refolding of a Protein with No Disulfide Bonds. The Journal of Biological Chemistry, 269(40), 24550-24552.

Chevet, Fessart, Delom, Mulot, Vojtesek, Hrstka, Murray, Gray and Hupp (2013) Emerging roles for the pro-oncogenic anterior gradient-2 in cancer Development. Oncogene, 32, 2499-2509.

Dumartin et al. (2011) AGR2 is a Novel Surface Antigen that Promotes the Dissemination of Pancreatic Cancer Cells through the Regulation of Cathepsins B and D. Cancer Research, 71, 7091-7102.

Ellgaard and Helenius (2001) ER quality control: towards an understanding at the molecular level. Current Opinion in Cell Biology, 13, 431-437.

Ellerman, Myles and Primakoff (2006) A Role for Sperm Surface Protein Disulfide Isomerase Activity in Gamete Fusion: Evidence for the Participation of ERp57. Developmental Cell, 10, 831-837.

Flaherty, Robert, Hersey, Nathan, Garbe, Milhem, Demidov, Hassel, Rutkowski, Mohr, Dummer, Trefzer, Larkin, Utikal, Dreno, Nyakas, Middleton, Becker, Casey, Sherman, Wu, Quellet, Martin, Patel and Schadendorf (2012) Improved Survival with MEK Inhibition in BRAF-Mutated Melanoma. New England Journal of Medicine, 367, 107-114.

Goplen, Wang, Enger, Tysnes, Terzis, Laerum and Bjerkvig (2006) Protein Disulfide Isomerase Expression is Related to the Invasive Properties of Malignant Glioma. Cancer Research, 66, 9895-9902.

Hauschild, Grob, Demidov, Jouary, Gutzmer, Millward, Rutkowski, Blank, Miller, Kaempgen, Martin-Algarra, Karaszewska, Mauch, Chiarion-Sileni, Martin, Swann, Haney, Mirakhur, Guckert, Goodman and Chapman (2012) Dabrafenib in BRAF-mutated metastatic melanoma: a multicentre, open-label, phase 3 randomised controlled trial. The Lancet, 9839(28), 358-365.

Higa, Mulot, Delom, Bouchecareilh, Nguyên, Boismenu, Wise and Chevet (2011) Role of Pro-oncogenic Protein Disulfide Isomerase (PDI) Family Member Anterior Gradient 2 (AGR2) in the Control of Endoplasmic Reticulum Homeostasis. Journal of Biological Chemistry, 52, 44855-44584.

Hrstka, Nenutil, Fourtouna, Maslon, Naughton, Langdon, Murray, Larionov, Petrakova, Muller, Dixon, Hupp and Vojtesek (2010) The pro-metastatic protein anterior gradient-2 predicts poor prognosis in tamoxifen-treated breast cancers. Oncogene, 29, 4838-4847.

Ikawa, Nakanishi, Yamada, Wada, Kominami, Tanaka, Nozaki, Nishimune and Okabe (2001) Calmegin Is Required for Fertilin α/β Heterodimerization and Sperm Fertility. Developmental Biology, 240(1), 254-261.

Ikawa, Tokuhiro, Yamaguchi, Benham, Tamura, Wada, Satouh and Inoue (2011) Calsperin Is a Testis-specific Chaperone Required for Sperm Fertility. The Journal of Biological Chemistry, 286(7), 5639-5646.

Landegren, Sharon, Freyhult, Hallgren, Eriksson, Edqvist, Bensing, Wahlber, Nelson, Gustafsson, Husebye, Anderson, Snyder and Kämpe (2016) Proteome-wide survey of the autoimmune target repertoire in autoimmune polyendocrine syndrome type 1. Scientific Reports 1(6), 20104.

Le Naour, Brichory, Misek, Bréchot, Hanash and Beretta (2002) A Distinct Repertoire of Autoantibodies in Hepatocellular Carcinoma Identified by Proteomic Analysis. Molecular & Cellular Proteomics, 1, 197-203.

Lovat, Corazzari, Armstrong, Martin, Pagliarini, Hill, Brown, Piacentini, Birch-Machin and Redfern (2008) Increasing Melanoma Cell Death Using Inhibitors of Protein Disulfide Isomerases to Abrogate Survival Responses to Endoplasmic Reticulum Stress. Cancer Research, 68, 5363-5369.

Masahiro, Kondoh, Imazeki, Tanaka, Okada, Mori, Hada, Arai, Wakatsuki, Matsubara, Yamamoto and Yamamoto (2003) Activation of the ATF6, XBP1 and grp78 genes in human hepatocellular carcinoma: a possible involvement of the ER stress pathway in hepatocarcinogenesis. Journal of Hepatology, 38(5), 605 – 614.

Meixia, Naczki, Koritzinsky, Fels, Blais, Hu, Harding, Novoa, Varia, Raleigh, Scheuner, Kaufman, Bell, Ron, Wouters and Koumenis (2005) ER stress-regulated translation increases tolerance to extreme hypoxia and promotes tumor growth. The EMBO Journal, 24, 3470-3481.

Merksamer and Papa (2010) The UPR and cell fate at a glance. Journal of Cell Science, 123, 1003-1006.

Mody and Mcilroy (2014) The mechanisms of Fenretinide-mediated anti-cancer activity and prevention of obesity and type-2 diabetes. Biochemical Pharmacology 91(3), 277-286.

Moenner, Pluquet, Bouchecareilh and Chevet (2007) Integrated Endoplasmic Reticulum Stress Response in Cancer. Cancer Research, 67, 10631-10634

Nawrocki, Carew, Dunner, Boise, Chiao, Huang, Abbruzzese and McConkey (2005) Bortezomib inhibits PKR-like endoplasmic reticulum (ER) kinase and induces apoptosis via ER stress in human pancreatic cancer cells. Cancer Research, 65(24), 11510-11519.

Olden, Corre, Hayward, Toniolo, Ulivi, Gasparini, Pistis, Hwang, Bergmann, Campbell, Cocca, Gandin, Girotto, Glaudemans, Hastie, Loffing, Polasek, Rampoldi, Rudan, Sala, Traqlia, Vollenweider, Vuckovic, Youhanna, Weber, Wright, Kutalik, Bochud, Fox and Devuysk (2014) Common variants in UMOD associate with urinary uromodulin levels: a meta-analysis. Journal of the American Society of Nephrology, 25(8, 1869-82.

Ozawa, Tsukamoto, Hori, Kitao, Yanagi, Stern and Ogawa (2001) Regulation of Tumor Angiogenesis by Oxygen-regulated Protein 150, an Inducible Endoplasmic Reticulum Chaperone. Cancer Research, 61(10), 4206–4213.

Ozcan and Tabas (2012) Role of Endoplasmic Reticulum Stress in Metabolic Disease and Other Disorders. Annual Review of Medicine, 63, 317–328.

Park, Zhen, Verhaeghe, Nakagami, Nguyenvu, Barczak, Kileen and Erle (2009) The protein disulfide isomerase AGR2 is essential for production of intestinal mucus. Proceedings of the National Academy of Sciences of the United States of America, 106(17), 6950–6955.

Samanta, Tamura, Dubeau, Mhawech-Fauceglia, Miyagi, Kato, Lieberman, Buckanovich, Lin, and Neamati (2017) Expression of protein disulfide isomerase family members correlates with tumor progression and patient survival in ovarian cancer. Oncotarget, 8(61), 103543-103556.

Smid, Wang, Klijn, Sieuwerts, Zhang, Atkins, Martens and Foekens (2006) Genes Associated With Breast Cancer Metastatic to Bone. Journal of Clinical Oncology, 24(15), 2261-2267.

Sosman, Klim, Schuchter, Gonzalez, Pavlick, Weber, McArthur, Hutson, Moschos, Flaherty, Hersey, Kefford, Lawrence, Puzanov, Lewis, Amaravadi, Chielowski, Lawrence, Shyr, Ye, Li, Nolop, Lee, Joe and Ribas (2012) Survival in BRAF V600–Mutant Advanced Melanoma Treated with Vemurafenib. New England Journal of Medicine, 366(8), 707-714.

Staub (2001) A Century of Research on Mammalian Male Germ Cell Meiotic Differentiation In Vitro. Journal of Andrology, 22(6), 911-926.

Szarka and Bánhegyi (2011) Oxidative folding: recent developments. Biomolecular Concepts, 2, 379-390.

Tokuhiro, Ikawa, Benham and Okabe (2012) Protein disulfide isomerase homolog PDILT is required for quality control of sperm membrane protein ADAM3 and male fertility. Proceedings of the National Academy of Sciences of the United States of America, 109(10), 3850-3855.

Tzimas, Chevet, Jenna, Nguyên, Khatib, Marcus, Zhang, Chrétien, Seidah and Metrakos (2005) Abnormal expression and processing of the proprotein convertases PC1 and PC2 in human colorectal liver metastases. BMC Cancer, 5, 149.

van Lith, Nartigan, Hatch and Benham (2005) PDILT, a Divergent Testis-specific Protein Disulfide Isomerase with a Non-classical SXXC Motif That Engages in Disulfide-dependent Interactions in the Endoplasmic Reticulum. The Journal of Biological Chemistry, 280(2), 1376-1383.

van Lith, Karala, Bown, Gatehouse, Ruddock, Saunders and Benham (2007) A Developmentally Regulated Chaperone Complex for the Endoplasmic Reticulum of Male Haploid Germ Cells. Molecular Biology of the Cell, 18, 2795-2804.

Watanabe, Yamada, Nishina, Tajima, Koshimizu, Nagata and Nishimune (1993) Molecular Cloning of a Novel Ca2+-binding Protein (Calmegin) Specifically Expressed during Male Meiotic Germ Cell Development. Journal of Biological Chemistry, 10, 7744-7749.

Watanabe, Laurindo and Fernandes (2014) Methods of measuring protein disulfide isomerase activity: a critical overview. Frontiers in Chemistry, 2, 73.

Welch (1992) Mammalian Stress Response: Cell Physiology, Structure/Function of Stress Proteins, and Implications for Medicine and Disease. Physiological Reviews, 72(4), 1063-1081.

Wilkinson (2004) Protein disulfide isomerase. Biochimica et Biophysica Acta, 1699, 35–44.

Yang, Wang, Niu, Li, Dong, Liu, Wang and Liang (2018) Crystal and solution structures of human protein-disulfide isomerase-like protein of the testis (PDILT) provide insight into its chaperone activity. Journal of Biological Chemistry. 293(4). 1192-1202.

Xu, Sankar and Neamati (2014) Protein Disulfide Isomerase: A Promising Target for Cancer Therapy. Drug Discovery, 19, 222-240.